AD-A056 365 ARMY ARMAMENT RESEARCH AND DEVELOPMENT COMMAND ABERD--ETC F/G 20/2
EFFECT OF DIFFERENT INITIAL ACCELERATIONS ON THE SUBSEQUENT SHO--ETC(U)
MAY 78 D F STRENZWILK

UNCLASSIFIED ARBRL-TR-02065 SBIE-AD-E430 059 NL

| OF |
AD
A056365

END
DATE
FILMED
8 -78
DDC

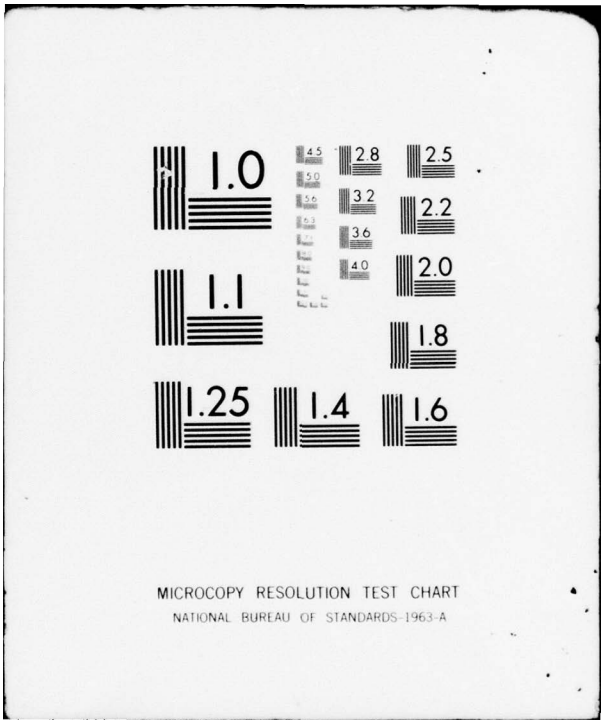
1.0
1.1
1.25
1.4
1.6
1.8
2.0
2.2
2.5
2.8
3.2
3.6
4.0
4.5
5.0
5.6
6.3
MICROCOPY RESOLUTION TEST CHART
NATIONAL BUREAU OF STANDARDS-1963-A

(12) LEVEL II

TECHNICAL REPORT ARBRL-TR-02065

EFFECT OF DIFFERENT INITIAL ACCELERATIONS ON THE SUBSEQUENT SHOCK PROFILE IN ONE-DIMENSIONAL LATTICES

Denis F. Strenzwilk

May 1978

US ARMY ARMAMENT RESEARCH AND DEVELOPMENT COMMAND
BALLISTIC RESEARCH LABORATORY
ABERDEEN PROVING GROUND, MARYLAND

Destroy this report when it is no longer needed.
Do not return it to the originator.

Secondary distribution of this report by originating or sponsoring activity is prohibited.

Additional copies of this report may be obtained from the National Technical Information Service, U.S. Department of Commerce, Springfield, Virginia 22161.

The findings in this report are not to be construed as an official Department of the Army position, unless so designated by other authorized documents.

The use of trade names or manufacturers' names in this report does not constitute indorsement of any commercial product.

UNCLASSIFIED

SECURITY CLASSIFICATION OF THIS PAGE (When Data Entered)

REPORT DOCUMENTATION PAGE	READ INSTRUCTIONS BEFORE COMPLETING FORM
1. REPORT NUMBER: TECHNICAL REPORT ARBRL-TR-02065	2. GOVT ACCESSION NO. / 3. RECIPIENT'S CATALOG NUMBER
4. TITLE (and Subtitle): Effect of Different Initial Accelerations on the Subsequent Shock Profile in One-Dimensional Lattices	5. TYPE OF REPORT & PERIOD COVERED: Technical Report / 6. PERFORMING ORG. REPORT NUMBER
7. AUTHOR(s): Denis F. Strenzwilk	8. CONTRACT OR GRANT NUMBER(s)
9. PERFORMING ORGANIZATION NAME AND ADDRESS: US Army Ballistic Research Laboratory (ATTN: DRDAR-BLB) Aberdeen Proving Ground, MD 21005	10. PROGRAM ELEMENT, PROJECT, TASK AREA & WORK UNIT NUMBERS: 1L161102AH43
11. CONTROLLING OFFICE NAME AND ADDRESS: US Army Armament Research & Development Command US Army Ballistic Research Laboratory ATTN: DRDAR-BL APG, MD 21005	12. REPORT DATE: MAY 1978 / 13. NUMBER OF PAGES: 73 (70 P.)
14. MONITORING AGENCY NAME & ADDRESS (if different from Controlling Office)	15. SECURITY CLASS. (of this report): Unclassified / 15a. DECLASSIFICATION/DOWNGRADING SCHEDULE

16. DISTRIBUTION STATEMENT (of this Report)

Approved for public release; distribution unlimited.

17. DISTRIBUTION STATEMENT (of the abstract entered in Block 20, if different from Report)

SBIE

AD-E 430 054

18. SUPPLEMENTARY NOTES

19. KEY WORDS (Continue on reverse side if necessary and identify by block number)

Shock Propagation, Lattice Dynamics, Computer Molecular Dynamics, Solitons
Envelope Solitons

20. ABSTRACT (Continue on reverse side if necessary and identify by block number) (hmn)

Shock propagation in a one-dimensional, discrete lattice is generated by accelerating the end-most particle from zero to its final velocity in a finite rise time after which the end particle is maintained at that velocity. The wave profiles for various rise times are compared to the zero-time case in a quiescent lattice. Analytical work is presented for the linear lattice, but for the anharmonic lattice the classical equations of motion of the atoms are solved numerically on the computer. A Morse-type potential is assumed. For a

→ next page

DD FORM 1 JAN 73 1473 EDITION OF 1 NOV 65 IS OBSOLETE

393 471

UNCLASSIFIED

SECURITY CLASSIFICATION OF THIS PAGE (When Data Entered)

finite rise time the amplitude of the wave passing through the surface atoms is diminished when compared with the zero-time case. For the anharmonic lattice the head of the wave develops into a solitary wave train with an oscillatory tail, and for certain rise times and anharmonicity parameters an envelope soliton forms behind the shock front. This envelope soliton travels much slower than the shock wave. The relevance to Army-related problems is discussed.

TABLE OF CONTENTS

LIST OF FIGURES

Figure Page

1. INTRODUCTION

Historically, the most common assumption for generating a shock wave in a lattice from a microscopic point of view is to maintain the end particle at a steady compression velocity u for all times. Paskin and Dienes[1-2], Manvi[3-6], Duvall[3-5], and Lowell[3-4], Tasi[7-12], and Musgrave[11-12], and Powell and Batteh[13] have used the above assumption while Beckett[14]

---

1. A. Paskin and G.J. Dienes, "Molecular Dynamic Simulations of Shock Waves in a Three-Dimensional Solid", J. Appl. Phys. 43, 1605 (1972).
2. A. Paskin and G.J. Dienes, "A Model for Shock Waves in Solids and Evidence for a Thermal Catastrophe", Solid State Comm. 17, 197 (1975).
3. R. Manvi, G.E. Duvall, and S.C. Lowell, "Finite Amplitude Longitudinal Waves in Lattices", Int. J. Mech. Sci. 11, 1 (1969).
4. G.E. Duvall, R. Manvi, and S.C. Lowell, "Steady Shock Profile in a One-Dimensional Lattice", J. Appl. Phys. 40, 3771 (1969).
5. R. Manvi, and G.E. Duvall, "Shock Waves in a One-Dimensional, Non-Dissipating Lattice", Brit. J. Appl. Phys. 2, 1389 (1969).
6. R. Manvi, "Shock Wave Propagation in a Dissipating Lattice Model", Ph.D. Thesis (Washington State University, 1968) (Unpublished).
7. J. Tasi, "Perturbation Solution for Growth of Nonlinear Shock Waves in a Lattice", J. Appl. Phys. 43, 4016 (1972). See also Erratum (J. Appl. Phys. 44, 1414 (1973)).
8. J. Tasi, "Perturbation Solution for Shock Waves in a Dissipative Lattice", J. Appl. Phys. 44, 2245 (1973).
9. J. Tasi, "Far-Field Analysis of Nonlinear Shock Waves in a Lattice", J. Appl. Phys. 44, 4569 (1973).
10. J. Tasi, "Reflection of Nonlinear Shock Waves in a Lattice", J. Appl. Phys. 47, 5336 (1976).
11. M.J.P. Musgrave and J. Tasi, "Shock Waves in Diatomic Chains - I. Linear Analysis", J. Mech. Phys. Solids 24 19 (1976).
12. J. Tasi and M.J.P. Musgrave, "Shock Waves in Diatomic Chains - II. Nonlinear Analysis", J. Mech. Phys. Solids 24, 43 (1976).
13. J. Powell and J. Batteh, "Shock Propagation in the One-Dimensional Lattice", BRL Report No. 2009, 1977. (AD #A044791)
14. D.H. Tsai and C.W. Beckett, "Shock Wave Propagation in Cubic Lattices", J. Geophys. Res. 71, 2601 (1966).

MacDonald[15], and Tsai[14-17] have assumed that it is more realistic to accelerate the end particle from zero to its final velocity in a time t_{max}. Indeed, it seems impossible for the end particle to achieve its final velocity instantaneously. There should be some effect on wave propagation in the surface atoms, and perhaps some other phenomena owing to the differences in the two cases. However, it is not clear whether the results will be changed enough to warrant the additional complications of a more realistic model. Therefore, the purpose of this report is to obtain a better understanding of wave propagation in a lattice for the two different cases. A fringe benefit of this study is that some results have been obtained for the most common assumption, which will be reported here for the first time.

The specific problem chosen for study in this report is a small part of an ever increasing research effort to describe shock propagation in solids from a microscopic point of view. Usually this nonlinear problem of solving Newton's second law for the motion of individual particles is done numerically on the computer. Since this method starts from such a fundamental equation, many physical effects can be treated without the usual simplifying assumptions of continuum mechanics. For instance, a well-known lattice-dynamical result predicts that if a one-dimensional lattice with linear interatomic forces is subjected to steady compression, the wave profile will spread as it travels farther into the lattice. This effect is explained by the fact that the normal-mode frequencies have different group velocities. However, this dispersion arising from the discrete nature of the lattice is not included in the hydrodynamic approach. Furthermore, when nonlinear interatomic forces are taken into account, the wave profile steepens and the normal modes of the crystal become coupled. The consequences of this coupling can best be determined by a microscopic approach.

Many physical effects are assumed in a continuum approach to have specific characteristics based on intuitive reasoning. One such assumption is that the shock compressed material has yielded completely, so that the stresses may be assumed to be hydrostatic. The usual justification for this statement is that the high pressure in the compressed region causes the shear-yielding to be complete. However, Tsai[15] has suggested

15. D.H. Tsai, "An Atomistic Theory of Shock Compression of a Perfect Crystalline Solid", in Accurate Characterization of the High-Pressure Environment, edited by E.C. Lloyd, Natl. Bur. Stds. Spec. Publ. No. 326 (U.S. GPO, Washington, DC, 1971), p. 105.
16. D.H. Tsai and R.A. MacDonald, "Second Sound in a Solid Under Shock Compression", J. Phys. C, 6, L171 (1973).
17. H. Prask, P. Kemmey, S. Trevino, D.H. Tsai, and S. Yip, "Computer Simulation Studies of the Microscopic Behavior of Shocked Solids", Proceedings of the Conference on Mechanisms of Explosion and Blast Waves, editor J. Alster (JTCG/ALNNO, Naval Weapons Station, Yorktown, VA, 1973, XVI).

that the yield strength of the material is probably much higher under dynamic conditions. This problem of time - dependent yielding under the transient condition of shock compression has not been exhaustively studied either experimentally or theoretically in the high-pressure regime. Furthermore, it is not clear if the steady state assumption, and thus the Hugoniot relationships in their usual form, apply. Other assumptions for continuum treatments of shock propagation concern the equation of state for the solid and the nature of viscous effects[18,19]. Actually, little is known about the equation of state, and the origins of viscous effects are not completely understood. In principle, by calculating the positions and velocities of the particles as a function of time in the microscopic approach, the quantities such as pressure, density, and temperature can be determined without an equation of state or assumed viscous effects.

Finally, nonlinear (anharmonic) lattice dynamics has been greatly influenced by the work of Fermi, Pasta and Ulam (FPU)[20]. At the time of their paper it was generally accepted that small nonlinearities would lead to equipartition of energy. In a linear (harmonic) system energy deposited into a normal mode can never flow to another normal mode, but it was thought that a small nonlinearity would cause energy to flow from one mode to another until the time-averaged energy of each mode was the same. FPU studied the vibration of particles connected by nonlinear springs by using a computer. They found that the system did not approach thermal equilibrium, but rather returned to its original state after a recurrence time. On the other hand, the hydrodynamic theory assumes that thermal equilibrium exists behind the shock and allows for only small deviations from equilibrium within the front. A recent report by Powell and Batteh[13] examines this question in some detail, including a discussion of the similarities and differences in the results and interpretations of earlier authors.

The approach to thermal equilibrium in the compressed region is important to the theory of detonation. For instance, the Zeldovich-von Neumann-Doring (ZND) theory of detonation[21] treats the shock front as a mathematical discontinuity. The only function of the shock wave is to provide the energy necessary to raise the temperature, density, and pressure of the lattice to values higher than in the undisturbed lattice. The condensed region, where chemical reactions occur, is assumed to be in thermodynamic equilibrium. However, numerical and perhaps analytical

18. W. Band, "Studies in the Theory of Shock Propagation in Solids", J. Geophys. Res. 65, 695 (1960).
19. D.R. Bland, "On Shock Structure in a Solid", J. Inst. Math. Applications 1, 56 (1965).
20. E. Fermi, J.R. Pasta, and S.M. Ulam, "Studies in Nonlinear Problems", Los Alamos Sci. Lab. Rep. LA-1940, 1955; also in Collected Works of Enrico Fermi (Univ of Chicago Press, Chicago, 1965), V. II, p. 978.
21 B.Lewis and G. von Elbe, Combustion, Flames and Explosion of Gases (Academic Press, New York, 1951), Chap. XI.

solutions may show that the shock profile is not steady, or the time to re-establish equilibrium is of the same order as of the time required for a chemical reaction. In that case some assumptions used in detonation theory will have to be changed.

2. THEORY

This model treats a semi-infinite chain of atoms, of mass m, which interact pairwise through a Morse potential. At equilibrium the lattice spacing between neighboring atoms is a_o, the displacement of the j^{th} atom from its equilibrium position is given by the coordinate x_j, the distance to the j^{th} atom from the origin of the system located at the equilibrium position of the zeroth atom is r_j, and the corresponding distance to the equilibrium position of the j^{th} atom is r_{oj}, (see Figure 1). The coordinates obey the relation,

$$r_j = r_{oj} + x_j \ . \tag{2.1}$$

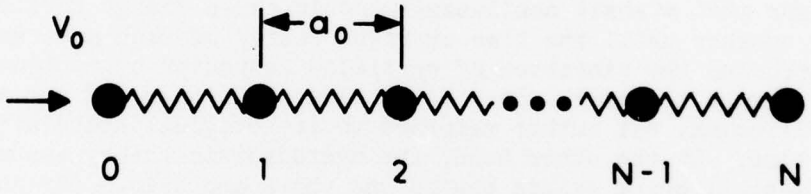

Figure 1. Model for simulating shock propagation in a one-dimensional discrete lattice.

The aim of this calculation is to obtain the solution for the classical equations of motion of the atoms when the zeroth atom is subjected to an acceleration which changes its velocity from zero to its final value u in a time t_{max}. Thereafter, the initial particle travels at a steady compression velocity u.

The Hamiltonian for the chain can be written as

$$H = \frac{1}{2} m \sum_{j=o}^{\infty} v^2_j + \Phi (r_1, r_2, \cdots, r_n) \ , \tag{2.2}$$

where $v_j = dx_j/dt$ is the velocity of the j^{th} particle and Φ is the total potential energy of the lattice. Newton's second law for the j^{th} particle becomes

$$m \frac{d^2 x_j}{dt^2} = F_j + F_j^{ext} \ , \tag{2.3}$$

where $F_j = -\frac{\partial \Phi}{\partial x_j}$ is the force exerted on the j^{th} particle by the remaining atoms of the lattice and F_j^{ext} is the corresponding external force. In this investigation, F_j^{ext} is zero for all particles except j=o, when it is varied in such a manner that this particle goes from zero velocity to the steady compression velocity u in a time t_{max}. It is the intention of this report to investigate the difference between the above F_o^{ext} and the more usual one which constrains the zeroth particle to move at constant velocity u for all times.

If we assume that Φ can be obtained by summing over two body potentials, i.e.,

$$\Phi(r_{01}, r_{02}, \cdots, r_{ij}, \cdots) = \sum_{i<j} \phi\,(|r_i - r_j|) \quad , \tag{2.4}$$

where $r_{ij} = r_i - r_j$, then ϕ can be expanded in a Taylor series about the equilibrium positions of the relative displacements, $r_{ij}^o = r_{oi} - r_{oj}$. Furthermore, if we assume that the deviations of the r_{ij} from their equilibrium value are small, the expansion can be truncated after second order terms such that

$$\Phi = \Phi_o(\cdots, r_{ij}^o, \cdots) + \frac{1}{2} \sum_{i,j=o} \phi_{ij}\, x_i x_j \quad , \tag{2.5}$$

where Φ_o is a constant which will arbitrarily be set equal to zero hereafter and where

$$\phi_{ij} = \left(\frac{\partial^2 \Phi}{\partial r_i \partial r_j} \right)_{r_{oi} r_{oj}} \quad . \tag{2.6}$$

The first-derivative term in the Taylor series expansion for the potential vanishes since it is the negative of the force on the j^{th} atom in the equilibrium configuration, which is zero. The potential in Eq. (2.5) is called the harmonic potential. Finally, if we assume only nearest-neighbor interactions such that only the $j+1^{st}$ and $j-1^{st}$ atom exert an appreciable force on the j^{th} atom, we have

$$\phi_{ij} = -\gamma(\delta_{i,j-1} - 2\delta_{ij} + \delta_{i,j+1}) \quad , \tag{2.7}$$

where γ is the force constant of the "spring" connecting successive particles and δ is the Kronecker δ. Equations (2.3)-(2.7) then imply that the equation of motion of the j^{th} particle is given in the harmonic approximation by

$$m \frac{d^2 x_j}{dt^2} = \gamma(x_{j+1} - 2x_j + x_{j-1}) + F_j^{ext}. \tag{2.8}$$

Equation (2.8) is a linear, second-order, differential equation and it has an exact analytic solution for certain external forces, which will be given later.

However, while Equation (2.8) can generally be used for calculating the equilibrium properties of a lattice especially at low temperatures, it is not a good starting point to describe a shock wave in a solid. The first reason is that at the high temperatures present in shock waves the relative displacements of the atoms from equilibrium are so large that higher order terms must be retained in Equation (2.5). Second, in the harmonic approximation the shock energy is initially distributed among the normal modes in a nonequilibrium fashion and there is no coupling mechanism allowing the crystal to thermalize after the shock has passed. Furthermore, the steepening of the wave profile in a compressed lattice is caused by the nonlinear terms. Therefore, the shock wave, which results from the steepening, must include nonlinear terms.

In the present research a Morse potential was used, and only nearest-neighbor interactions were assumed. The Morse potential can be written as

$$\Phi_M = D \sum_{i=1}^{\infty} \left[e^{-a(x_i - x_{i-1})} - 1 \right]^2 , \tag{2.9}$$

where D, and a are constants which are usually fit to the experimental data.

3. THE HARMONIC LATTICE

A harmonic lattice cannot support a shock wave in the usual sense for the reasons given in the preceding section. However, the calculation was performed to gain a better physical understanding of the analogous nonlinear case. In addition, the calculations for the anharmonic case must reduce to the harmonic case as the nonlinear terms go to zero.

We shall begin by presenting the solution of Schroedinger[22] for the

22. E. Schroedinger, "Zur Dynamik Elastisch Gekoppelter Punktsysteme", Ann. Phys. 44, 916 (1914).

equations of motion for the atoms of an infinite, one-dimensional, harmonic lattice for arbitrary initial conditions. When the lattice is in equilibrium neighboring atoms are uniformly separated a distance a_o, where the zeroth atom is located at the origin (see Figure 2). All the external forces are zero. By observing the symmetry of the problem we can choose the initial velocities and positions of the particles for $j \leq 1$ so that the zeroth particle travels to the right in a prescribed manner. The result of the above selection is to change the boundary-value problem for wave propagation in a semi-infinite lattice to an initial-value problem for an infinite chain. We then use this model to investigate wave propagation for two sets of boundary conditions on the zeroth particle. In the first case, the zeroth particle is set in motion at constant velocity u, and in the second case it is accelerated from zero to its final velocity u in a time t_{max} after which it moves at constant velocity u.

3.1 General Solution of the Equations of Motion for the Semi-Infinite, One-Dimensional, Harmonic Chain with Boundary Conditions.

Consider a chain consisting of N atoms (see Figure 2) connected by harmonic springs of force constant γ. Every atom has mass m and is labeled by index j

$$-\frac{N-1}{2} \leq j \leq \frac{N-1}{2} \quad .$$

We will assume for convenience that N is odd. It will be made arbitrarily large in the final results.

The differential equation of motion for the j^{th} atom, assuming only nearest-neighbor interactions, is given by Eq. (2.8) without the forcing term, viz.,

$$m \frac{d^2 x_j}{dt^2} = \gamma(x_{j+1} - 2x_j + x_{j-1}). \tag{3.1}$$

As $N \to \infty$ Morse and Ingard[23] give the Schroedinger solution[22] in our notation as

23. P.M. Morse and K.U. Ingard, Theoretical Acoustics (McGraw-Hill, New York, 1968). Chap. 3.

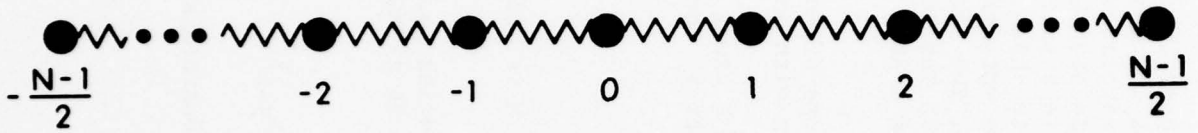

Figure 2. Model for solving the equations of motion for a one-dimensional, discrete lattice.

$$x_j(t) = \sum_{p=-\infty}^{\infty} \left\{ a_p \, J_{2j-2p}(\omega_o t) + \left(\frac{2}{\omega_o} \sum_{m=p+1}^{\infty} V_m \right) J_{2j-2p-1}(\omega_o t) \right\}, \qquad (3.2)$$

and

$$\frac{dx_j(t)}{dt} = \sum_{p=-\infty}^{\infty} \left\{ V_p \, J_{2j-2p}(\omega_o t) + \frac{1}{2} \omega_o (a_p - a_{p+1}) J_{2j-2p-1}(\omega_o t) \right\}, \qquad (3.3)$$

where a_p, V_p are the initial displacement and velocity at time t=o, $J_m(\omega_o t)$ are the Bessel functions of the first kind, of order m, and $\omega_o = 2\sqrt{\frac{\gamma}{m}}$.

We can guess from symmetry considerations the initial conditions which must be imposed on the particles $j \leq -1$ in order that the zeroth particle has the equation of motion $x_o = ut$ for all time. Consider an observer in a frame of reference moving at velocity u which is located at the origin of our stationary system at time t=o. If the initial conditions of the particles $j \geq 1$ are the mirror image of the particles $j \leq -1$ in this moving system, there will be no force on the zeroth particle. Therefore, we assume the following initial conditions,

$$-a_{-|j|} = a_{|j|}, \; V_{-|p|} = 2u - V_{|p|}, \; a_o = 0, \; V_o = u \quad . \qquad (3.4)$$

It can be shown that

$$\sum_{m=p+1}^{\infty} V_m = 2u|p| - u + \sum_{m=|p|}^{\infty} V_m \, , \; p \leq o \quad . \qquad (3.5)$$

Rearrangement of Eq. (3.2) using Eq. (3.4) and Eq. (3.5) results in the solution to the semi-infinite chain with the boundary condition $x_o = ut$, viz.,

$$x_j(t) = \sum_{p=1}^{\infty} \left\{ a_p \left(J_{2j-2p}(\omega_o t) - J_{2j+2p}(\omega_o t) \right) + \frac{2}{\omega_o} \left(\sum_{m=p}^{\infty} V_m \right) \left(J_{2j+2p-1}(\omega_o t) + J_{2j-2p+1}(\omega_o t) \right) + \frac{2u}{\omega_o} (2p-1) \, J_{2j+2p-1}(\omega_o t) \right\}, \; j \geq o \qquad (3.6)$$

and

$$\frac{dx_j(t)}{dt} = \frac{\omega_o}{2} \sum_{p=o}^{\infty} (a_p - a_{p+1}) \left(J_{2j-2p-1}(\omega_o t) + J_{2j+2p+1}(\omega_o t) \right)$$

$$+ \sum_{p=o}^{\infty} \left(V_p \, J_{2j-2p}(\omega_o t) + (2u - V_p) \, J_{2j+2p}(\omega_o t) \right)$$

$$- u \, J_{2j}(\omega_o t) \ , \ j \geq o \tag{3.7}$$

where the following relationship has been used

$$\frac{d}{dt} \, J_m(\omega_o t) = \frac{\omega_o}{2} \left(J_{m-1}(\omega_o t) - J_{m+1}(\omega_o t) \right) \ . \tag{3.8}$$

Other useful relationships of Bessel functions are

$$J_{-m}(\omega_o t) = (-1)^m \, J_m(\omega_o t), \ m \text{ integer} \tag{3.9a}$$

$$1 = \sum_{m=-\infty}^{\infty} J_{2m}(\omega_o t) = J_o(\omega_o t) + 2 \sum_{m=1}^{\infty} J_{2m}(\omega_o t) \ , \tag{3.9b}$$

$$\omega_o t = 2 \sum_{m=o}^{\infty} (2m+1) \, J_{2m+1}(\omega_o t) \ , \tag{3.9c}$$

and

$$J_m(o) = \delta_{om} \ . \tag{3.9d}$$

With the above relationships one can easily verify that $x_j(o) = a_j$, $\dot{x}_j(o) = V_j$.

From Eq. (3.6) and Eq. (3.9c) one can show that

$$x_o(t) = \frac{2u}{\omega_o} \sum_{p=o}^{\infty} (2p+1) \, J_{2p+1}(\omega_o t) = ut \ , \tag{3.10}$$

which is the correct boundary condition.

A special solution of Eq. (3.6) used in this investigation for the quiescent lattice, (a_j=o, V_j=o for j > o, V_o= u), is

$$x_j(t) = \frac{2u}{\omega_o} \sum_{p=o}^{\infty} (2p+1)\, J_{2j+2p+1}(\omega_o t) \quad . \tag{3.11}$$

Another special solution used in this investigation of the semi-infinite chain with the boundary condition $x_o = ut - \frac{ut_{max}}{2}$, $t \geqslant t_{max}$ can be determined by making the following observations. Let

$$Y_j(\bar{t}) = x_j(\bar{t}) - \frac{ut_{max}}{2} \quad , \tag{3.12}$$

where $\bar{t} = t - t_{max}$ so that the initial conditions at $\bar{t}$=o are

$$Y_o(o) = o,\ \dot{Y}_o(o)=u,\ Y_j(o)=a_j - \frac{ut_{max}}{2} \quad ,$$

and

$$\dot{Y}_j(o)=V_j, (j > o) \quad , \tag{3.13}$$

where a_j and V_j are the position and velocity of the j^{th} particle at $\bar{t}$=o.

$Y_j(\bar{t})$ satisfies an equation of the same form as Eq. (3.1), and has the same initial conditions at $\bar{t}$=o as $x_j(o)$ in Eq. (3.6). Therefore, the solution for $x_o = ut - \frac{ut_{max}}{2}$ is

$$\begin{aligned} x_j(t-t_{max}) = \sum_{p=1}^{\infty} \Bigg\{ & \left(a_p - \frac{ut_{max}}{2} \right) \left[J_{2j-2p}\left(\omega_o(t-t_{max})\right) - J_{2j+2p}\left(\omega_o(t-t_{max})\right) \right] \\ & + \frac{2}{\omega_o} \left(\sum_{m=p}^{\infty} V_m \right) \left[J_{2j+2p-1}\left(\omega_o(t-t_{max})\right) \right. \\ & \left. + J_{2j-2p+1}\left(\omega_o(t-t_{max})\right) \right] \\ & + \frac{2u}{\omega_o} (2p-1)\, J_{2j+2p-1}\left(\omega_o(t-t_{max})\right) \Bigg\} + \frac{ut_{max}}{2} \quad , t \geqslant t_{max} \end{aligned} \tag{3.14}$$

and

$$\frac{dx_j(t-t_{max})}{dt} = \frac{\omega_o}{2} \sum_{p=o}^{\infty} (a_j - a_{j+1}) \left[J_{2j-2p-1}\left(\omega_o(t-t_{max})\right) + J_{2j+2p+1}\left(\omega_o(t-t_{max})\right) \right] + \sum_{p=o}^{\infty} \left\{ V_p \, J_{2j-2p}\left(\omega_o(t-t_{max})\right) + (2u-V_p) \, J_{2j+2p}\left(\omega_o(t-t_{max})\right) \right\} - u \, J_{2j}\left(\omega_o(t-t_{max})\right),$$

$$t \geq t_{max} \quad . \tag{3.15}$$

The above solutions are matched at $t=t_{max}$ to the solutions which have a different boundary condition between $t=o$ and $t=t_{max}$.

Let us now consider a special solution to Eq. (3.1) with the following initial conditions at $t=o$, viz., $a_j=0$, $v_o=0$, $v_{|j|}$ are arbitraty, and $v_{-|j|}$ are to be determined, with the boundary condition

$$x_o = \frac{ut}{2} - \frac{ut_{max}}{2\pi} \sin\left(\frac{\pi t}{t_{max}}\right), \quad 0 \leq t \leq t_{max} \tag{3.16}$$

and

$$\frac{dx_o}{dt} = \frac{u}{2} - \frac{u}{2} \cos\left(\frac{\pi t}{t_{max}}\right) . \tag{3.17}$$

Under these conditions Eq. (3.3) and Eq. (3.17) reduces to

$$\frac{u}{2}\left(1-\cos\left(\frac{\pi t}{t_{max}}\right)\right) = \sum_{p=1}^{\infty} (V_p + V_{-p}) \, J_{2p}(\omega_o t) \quad , \tag{3.18}$$

where the V_{-p} are to be determined for arbitrary V_p. The $\cos\left(\frac{\pi t}{t_{max}}\right)$ has an expansion[24] in terms of Bessel functions depending on the range $\frac{\pi}{t_{max}\omega_o}$, viz.,

24. Handbook of Mathematical Functions, edited by M. Abramowitz and I. Stegun (Nat'l Bur. Std., WASH, DC, 1964), Chap. 9).

$$\cos(\omega_o t \sin\beta) = J_o(\omega_o t) + 2 \sum_{n=1}^{\infty} J_{2n}(\omega_o t) \cos 2n\beta, \qquad (3.19)$$

for the case $\frac{\pi}{t_{max}\omega_o} \leqslant 1$ where $\sin\beta = \frac{\pi}{t_{max}\omega_o}$

and

$$\cos(\omega_o t \cosh\alpha) = J_o(\omega_o t) + 2 \sum_{k=1}^{\infty} (-1)^k J_{2k}(\omega_o t) \cosh 2k\alpha, \qquad (3.20)$$

for the case $\frac{\pi}{t_{max}\omega_o} \geqslant 1$ where $\cosh\alpha = \frac{\pi}{t_{max}\omega_o}$. With the aid of Eq. (3.9b) and the above equations, Eq. (3.18) can be written as

$$\sum_{p=1}^{\infty} (V_p + V_{-p}) J_{2p}(\omega_o t) = \left\{ \begin{array}{l} u \sum_{p=1}^{\infty} (1-\cos 2p\beta) J_{2p}(\omega_o t) \\ \\ u \sum_{p=1}^{\infty} (1-(-1)^p \cosh 2p\alpha) J_{2p}(\omega_o t) \; . \end{array} \right\} \qquad (3.21)$$

$\frac{dx_o}{dt}$ is an example of an entire function. Therefore, it has a unique Neumann's expansion. We can conclude that the relationship between the arbitrary V_p and the determined V_{-p} is

$$V_p + V_{-p} = \left\{ \begin{array}{ll} u(1-\cos 2p\beta), & \frac{\pi}{t_{max}\omega_o} \leqslant 1 \\ \\ u(1-(-1)^p \cosh 2p\alpha), & \frac{\pi}{t_{max}\omega_o} \geqslant 1 \; . \end{array} \right. \qquad (3.22)$$

A note of caution is appropriate at this point. If one tries to obtain Eq. (3.22) by multiplying Eq. (3.18) by

$$\frac{J_{2p'}(\omega_o t)}{\omega_o t}$$

and then integrating from 0 to ∞ with the aid of Kapteyn's orthogonality relation[25],

25. W. Kapteyn, "Sur Quelques Integrales Definies Contenant Des Fonctions De Bessel", Archives Neerlandaises Des Sciences Exactes et Naturelles, VI, 103 (1901).

$$\int_0^\infty e^{-xt} \frac{J_n(t)}{t} dt = \frac{1}{n}\left(\sqrt{x^2+1} - x \right)^n , \quad n > 1 \tag{3.23}$$

a different result is obtained. This procedure requires a questionable interchange of two limit operations, one being the infinite series, the other the infinite (improper) integral. Apparently Eq. (3.20) is not uniformly convergent as pointed out by Gautschi[26]. The following summations are used for the final solution, viz.,

$$\sum_{m=1}^{p} \cos(2m\beta) = \frac{\sin[(2p+1)\beta]}{2 \sin \beta} - \frac{1}{2} , \tag{3.24}$$

and

$$\sum_{m=1}^{p} (-1)^m \cosh(2m\alpha) = \frac{(-1)^p \cosh(2p+1)\alpha - \cosh\alpha}{2 \cosh \alpha} . \tag{3.25}$$

Therefore, the solution to Eq. (3.1) for a semi-infinite chain with the boundary condition Eq. (3.16), and the initial conditions

$$a_{j=0}, \; {}^{V}|j|=0 ; \tag{3.26}$$

is

$$x_j(t) = \frac{2u}{\omega_o} \sum_{p=o}^{\infty} J_{2j+2p+1}(\omega_o t) \left\{ (p+\tfrac{1}{2}) - \left\{ \begin{array}{ll} \dfrac{\sin[(2p+1)\beta]}{2\sin\beta}, & \dfrac{\pi}{t_{max}\omega_o} \leq 1 \\ \dfrac{(-1)^p \cosh(2p+1)\alpha}{2 \cosh \alpha}, & \dfrac{\pi}{t_{max}\omega_o} \geq 1 \end{array} \right\} \right\} \tag{3.27}$$

and

$$\frac{dx_j(t)}{dt} = u \sum_{p=1}^{\infty} \left\{ \begin{array}{ll} (1-\cos 2p\beta), & \dfrac{\pi}{t_{max}\omega_o} \leq 1 \\ (1-(-1)^p \cosh 2p\alpha), & \dfrac{\pi}{t_{max}\omega_o} \geq 1 \end{array} \right\} J_{2j+2p'}(\omega_o t) . \tag{3.28}$$

26. W. Gautschi, private communication.

Eq. (3.27) and Eq. (3.28) at $t=t_{max}$ become the initial conditions a_j, V_j for Eq. (3.14) and Eq. (3.15), viz.,

$$a_j = x_j(t_{max}) \ , \tag{3.29}$$

and

$$V_j = \frac{dx_j(t_{max})}{dt} \ . \tag{3.30}$$

We now have the matched solution for a semi-infinite chain whose end particle is accelerated in a prescribed manner from zero to constant velocity u in time t_{max}.

3.2 Propagation in the Initially Quiescent Lattice.

If we assume that initially all particles except the first, which travels at velocity u (x_o=ut), are at rest in their equilibrium positions, we have Eq. (3.11). The velocity of the j^{th} particle is

$$\frac{dx_j(t)}{dt} = u\, J_{2j}(\omega_o t) + 2u \sum_{p=1}^{\infty} J_{2j+2p}(\omega_o t) \ . \tag{3.31}$$

The infinite series in Eq. (3.11) and Eq. (3.31) converge rapidly, and a computer program was written to evaluate the sums.

In Figure 3, we have plotted the nondimensionalized velocity and displacement of the 10^{th} particle as a function of nondimensionalized time, i.e.,

$$s_j(\tau) = \frac{\omega_o}{u} x_j(t), \ \frac{ds_j(t)}{d\tau} = \frac{1}{u} \frac{dx_j(t)}{dt} \ , \quad \tau=\omega_o t \ . \tag{3.32}$$

The peak velocity of the wave disturbance arrives at the 10^{th} particle at a rate of one half particle per unit of nondimensional time. This result is the maximum normal - mode velocity as can be obtained from the dispersion relation for the harmonic lattice, viz.,

$$\omega(k) = \omega_o \left|\sin \frac{ka_o}{2}\right| \tag{3.33}$$

where $\omega(k)$ is the frequency of the normal mode with wave vector k. The group velocity is

$$\frac{d\omega(k)}{dk} = \frac{\omega_o a_o}{2} \left|\cos \frac{ka_o}{2}\right| , \tag{3.34}$$

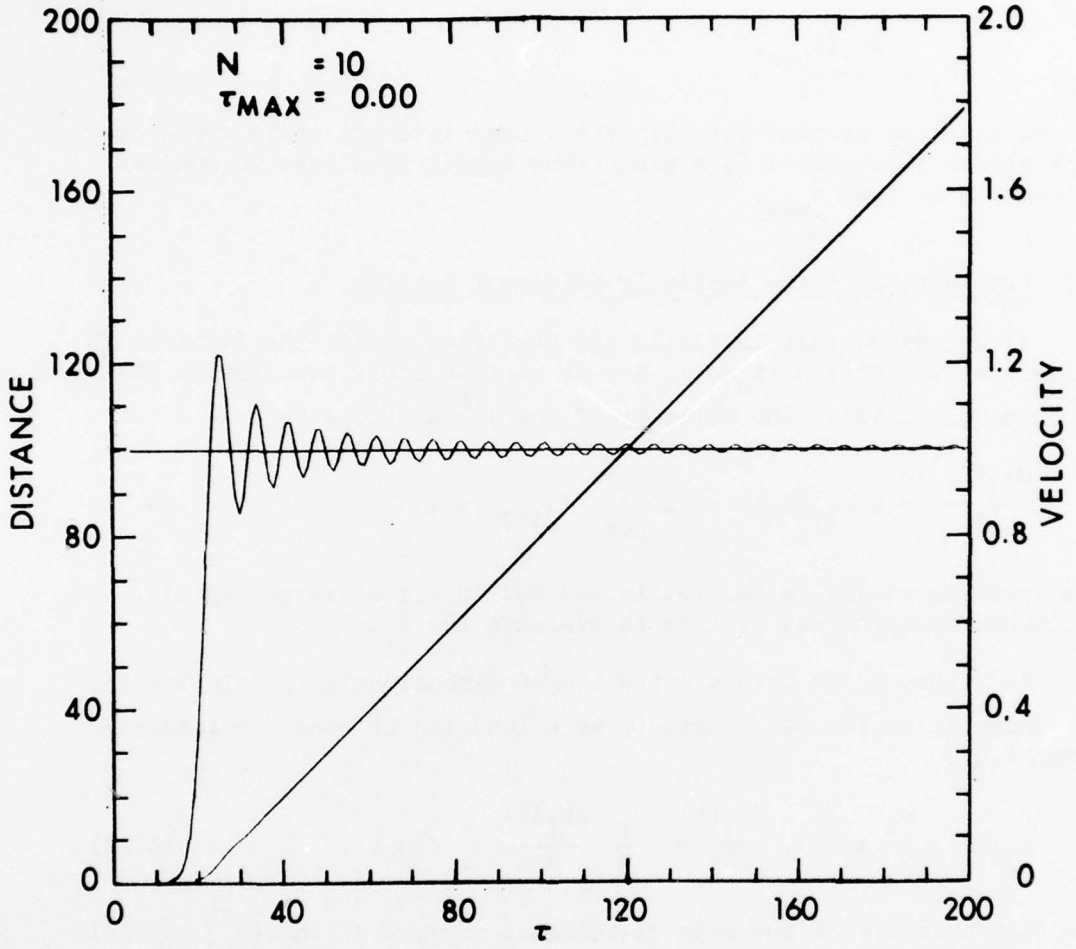

Figure 3. In dimensionless units the velocity which oscillates about unity and the displacement from equilibrium of the 10^{th} particle are plotted as a function of time for a harmonic lattice with a rise time $\tau_{max}=0.0$.

where the maximum is given by

$$\frac{d\omega(k)}{dk}\Big|_{max} = \frac{\omega_o a_o}{2} \quad . \tag{3.35}$$

Per unit of nondimensionalized time $\tau=\omega_o t$, the speed is $a_o/2$, or one half lattice spacing per unit tau. At a later time the wave has reached the 60^{th} particle, as can be seen in Fig. 4. The dispersive nature of the wave is evident.

The results for all cases where $t_{max} \neq 0.0$ are obtained from Eq. (3.27) and Eq. (3.28) for $t \leq t_{max}$, and from Eq. (3.14) and Eq. (3.15) for $t > t_{max}$. When the rise time $t_{max}=1.0$, we notice little difference in Figure 5 from the case $t_{max}=0$ in Figure 3. For a rise time $t_{max}=6.0$ we notice that each amplitude of the successive peaks in the wave train at the 10^{th} particle in Figure 6 is less than the corresponding amplitude at the 10^{th} particle in Figure 3. When this wave reaches the 60^{th} particle in Figure 7, each amplitude is not so great as the corresponding amplitude at the 60^{th}particle in Figure 4. This trend continues as the rise time increases. For a rise time $t_{max}=12.00$ each amplitude in the wave train for the 10^{th} particle in Figure 8 is very low. By the time the wave reaches the 60^{th} particle in Figure 9 its amplitudes are much smaller than at the 60^{th} particle in Figure 4. When the wave reaches the 140^{th} particle in Figure 10, it still does not have the amplitudes of the 60^{th} particle in Figure 4, although its amplitudes have increased from their value at the 60^{th} particle in Figure 9.

Now we can make some general observations about the velocity-time trajectories at specific particles near the surface in the harmonic approximation. Each amplitude of the successive peaks in the wave train is less than the corresponding amplitude for the instantaneous compression case by an amount which is inversely proportional to the rise time τ_{max}. This phenomenon most likely results from the fact that the total computed work done on the zeroth particle at the time when the first velocity peak is at a specific particle is less than the corresponding instantaneous acceleration case. Therefore, surface effects will persist for hundreds of atoms if the rise times are large enough. It should be pointed out that wave propagation in a quiescent harmonic lattice has more applicability to propagation on a thermal background than one might at first suspect. Powell and Batteh[13] have concluded that in a harmonic lattice the ensemble average taken over many initial conditions will lead to the same results for the average velocity and displacement as for the case in which the initial conditions are zero.

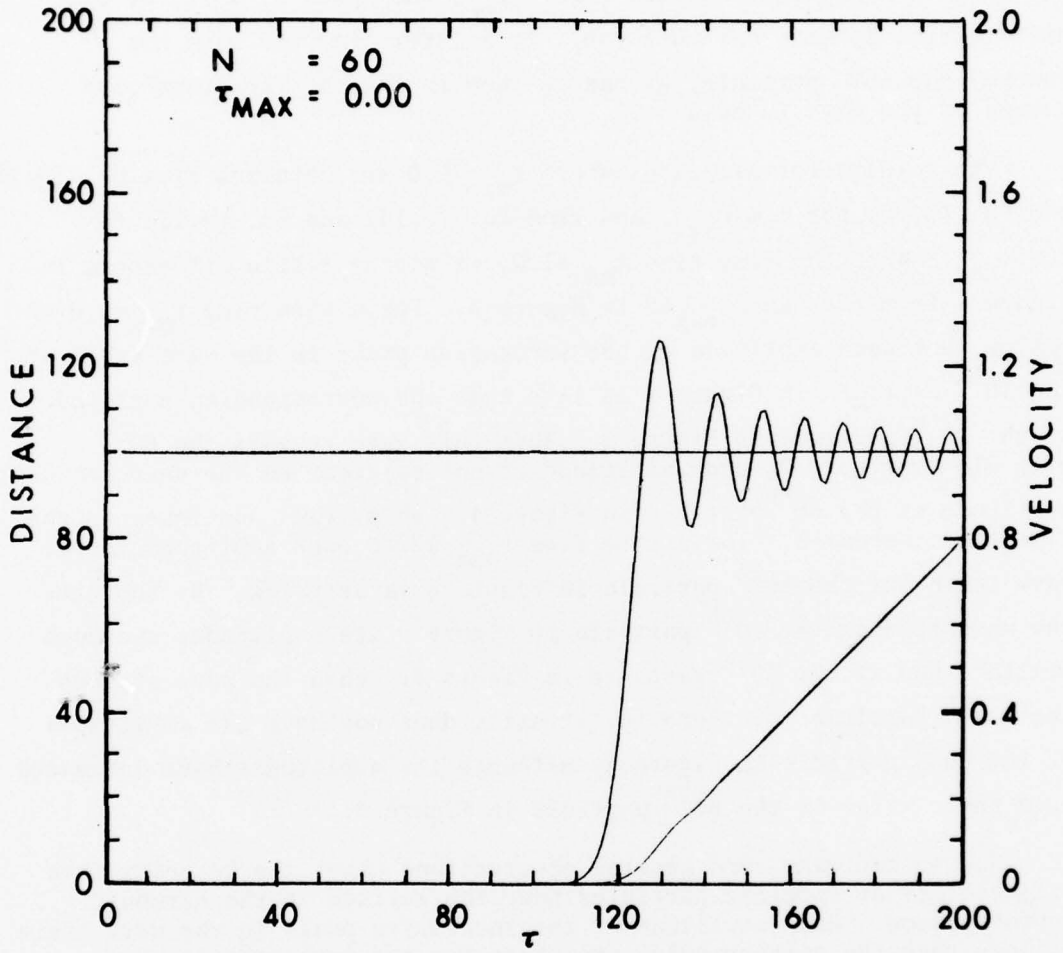

Figure 4. In dimensionless units the velocity which oscillates about unity and the displacement from equilibrium of the 60th particle are plotted as a function of time for a harmonic lattice with a rise time τ_{max}=0.0.

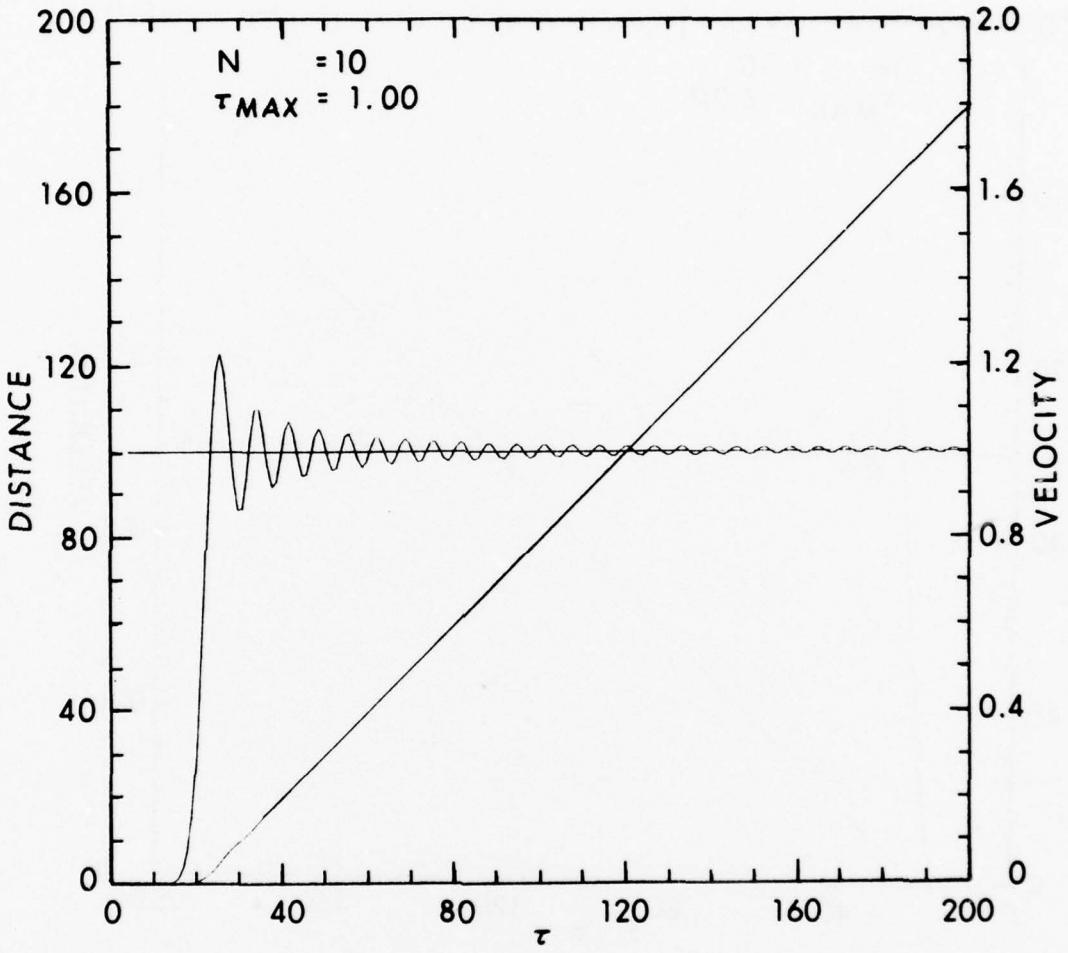

Figure 5. In dimensionless units the velocity which oscillates about unity and the displacement from equilibrium of the 10^{th} particle are plotted as a function of time for a harmonic lattice with a rise time τ_{max}=1.0.

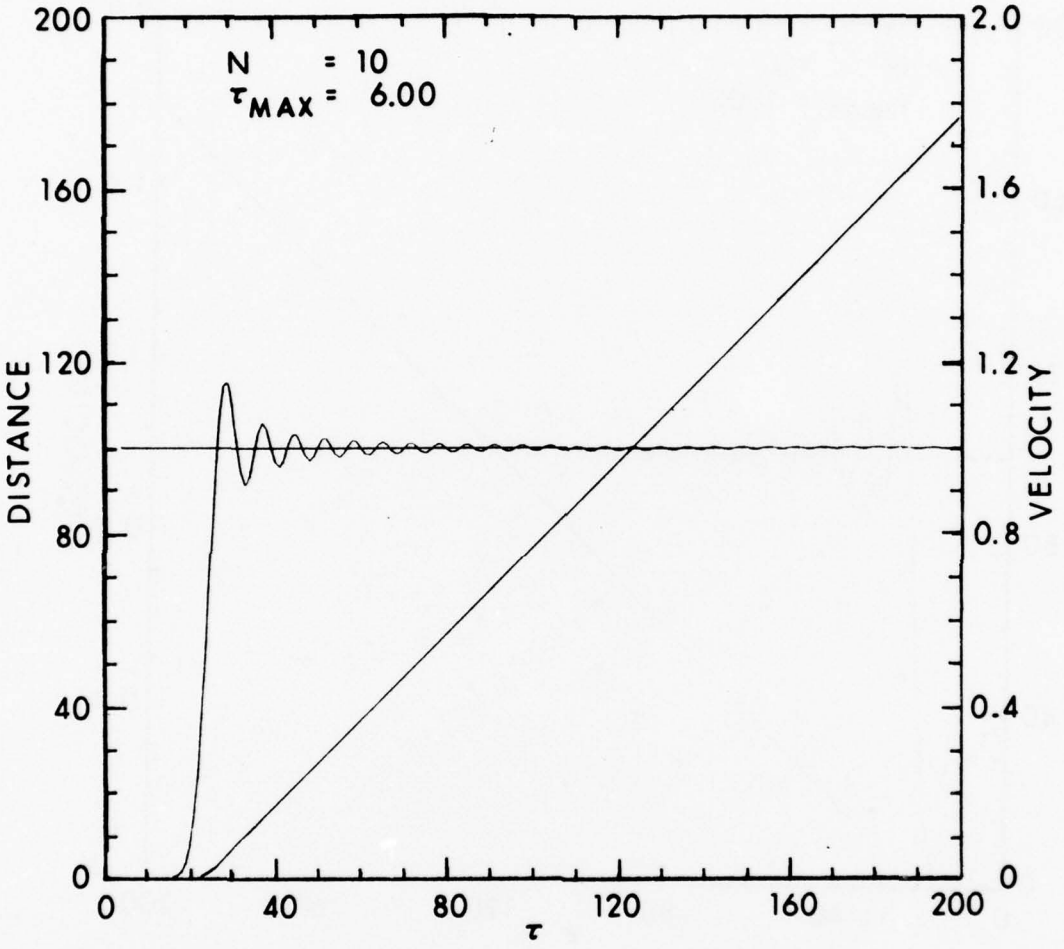

Figure 6. In dimensionless units the velocity which oscillates about unity and the displacement from equilibrium of the 10^{th} particle are plotted as a function of time for a harmonic lattice with a rise time τ_{max}=6.0.

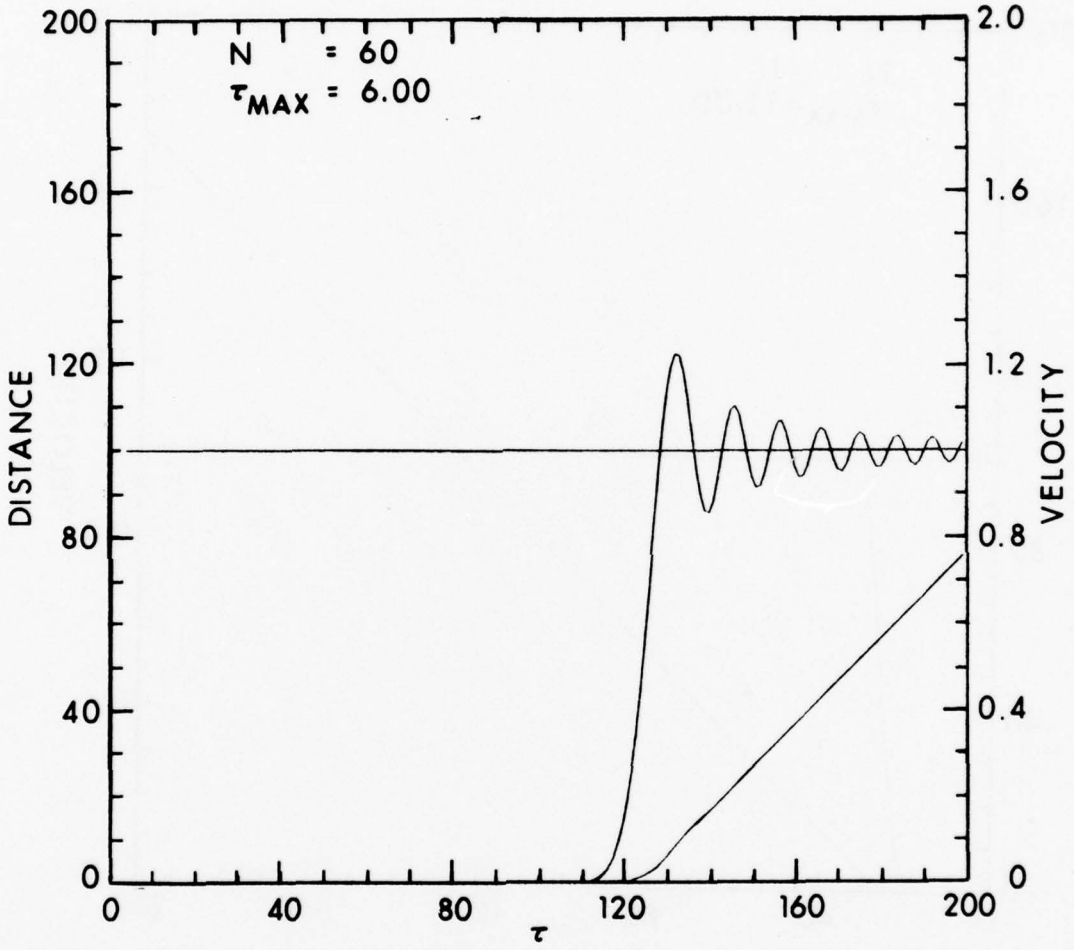

Figure 7. In dimensionless units the velocity which oscillates about unity and the displacement from equilibrium of the 60th particle are plotted as a function of time for a harmonic lattice with a rise time τ_{max}=6.0.

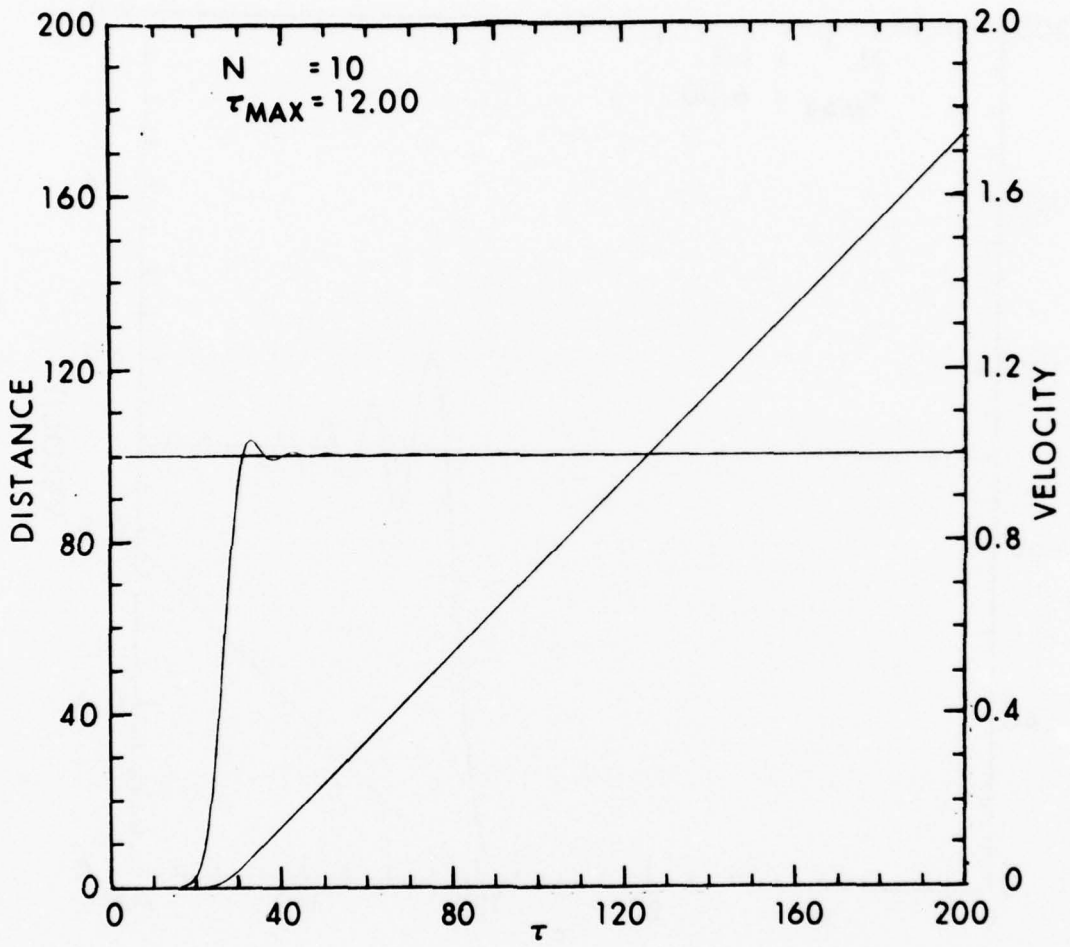

Figure 8. In dimensionless units the velocity which oscillates about unity and the displacement from equilibrium of the 10^{th} particle are plotted as a function of time for a harmonic lattice with a rise time τ_{max}=12.00.

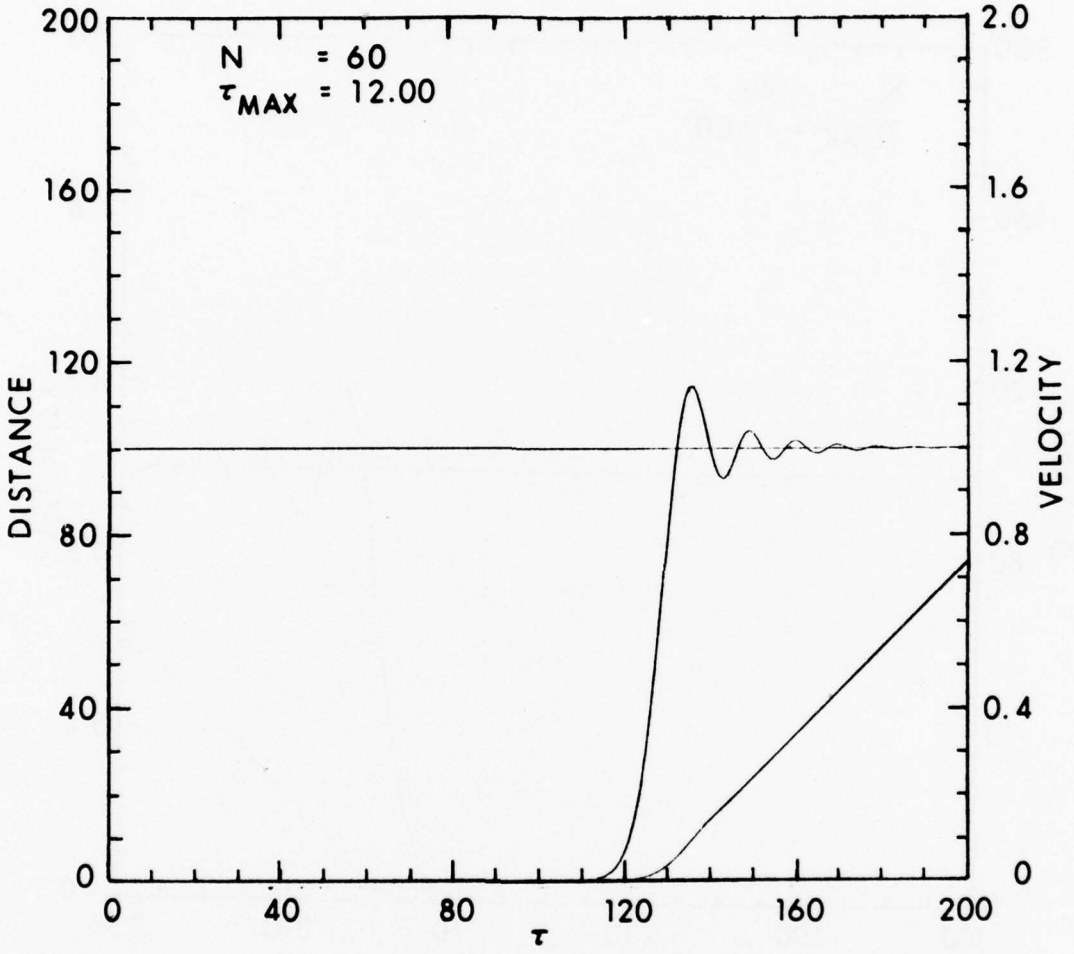

Figure 9. In dimensionless units the velocity which oscillates about unity and the displacement from equilibrium of the 60th particle are plotted as a function of time for a harmonic lattice with a rise time τ_{max}=12.00.

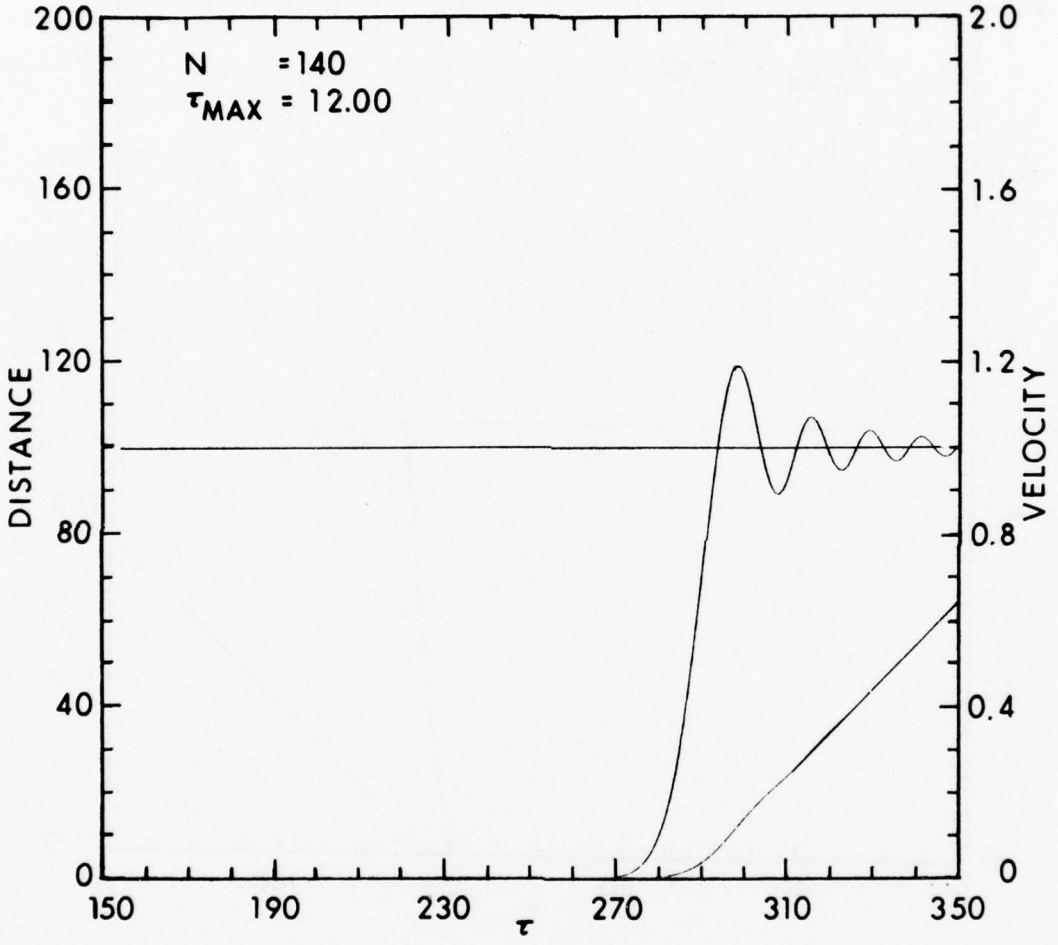

Figure 10. In dimensionless units the velocity which oscillates about unity and the displacement from equilibrium of the 140^{th} particle are plotted as a function of time for a harmonic lattice with a rise time τ_{max}=12.00.

4. NONDIMENSIONALIZED EQUATIONS FOR ANHARMONIC CASE AND METHOD FOR SOLUTION

If the Morse potential of Eq. (2.9) is used in Newton's second law of Eq. (2.3), and F_j^{ext} is set to zero, we can obtain the nondimensionalized equations of motion, viz.,

$$\frac{d^2 s_j(\tau)}{d\tau^2} = \frac{1}{4A_m}\left[\exp\left\{-A_m(s_{j+1}-s_j)\right\} - \exp\left\{-2A_m(s_{j+1}-s_j)\right\} - \exp\left\{-A_m(s_j-s_{j-1})\right\} + \exp\left\{-2A_m(s_j-s_{j-1})\right\}\right], j \geq 1 \tag{4.1}$$

where the definitions in Eq. (3.32) are used as well as

$$A_m = \frac{a\alpha}{\omega_o}, \quad D = \frac{m\omega_o^2}{8a^2} \quad . \tag{4.2}$$

The boundary condition for the zeroth particle can be chosen as desired. In this paper three cases are investigated,

$$s_o = \tau, \ \tau \geq 0 \tag{4.3a}$$

$$\left.\begin{aligned} s_o &= \frac{1}{2}\left(\tau - \frac{\tau_{max}}{\pi}\sin\left(\frac{\pi\tau}{\tau_{max}}\right)\right), \ 0 \leq \tau \leq \tau_{max} \ ; \\ s_o &= \tau - 1/2\ \tau_{max}, \ \tau > \tau_{max} \end{aligned}\right\} \tag{4.3b}$$

$$s_o = \frac{\tau^2}{2\tau_{max}}, \ 0 \leq \tau \leq \tau_{max}; \ s_o = \tau - 1/2\ \tau_{max}, \ \tau > \tau_{max} \tag{4.3c}$$

where $\tau_{max} = \omega_o t_{max}$.

Eq. (4.1) and Eq. (4.3) constitute a set of N coupled, nonlinear, second-order differential equations which must be solved numerically for various values of the parameters under consideration. These equations can be converted to a set of 2n first order equations, viz.,

$$\begin{aligned} \dot{s}_j &= v_j \\ \dot{v}_j &= \frac{1}{4A_m}\left\{ \exp\left[-2A_m(s_j-s_{j-1})\right] - \exp\left[-A_m(s_j-s_{j-1})\right] - \exp\left[-2A_m(s_{j+1}-s_j)\right] + \exp\left[-A_m(s_{j+1}-s_j)\right]\right\}, j \geq 1 \\ \dot{v}_o &= \frac{d^2 s_o}{d\tau^2} \ , \end{aligned} \tag{4.4}$$

where the dot denotes differentiation with respect to the dimensionless time τ.

To solve Eq. (4.4) we employed a computer program developed by Powell and Batteh[13], modified to take into account the different boundary conditions in Eq. (4.3). This program uses a fourth-order Runge-Kutta scheme[27]. Given the values of the functions on the left-hand side of Eq. (4.4) at time τ, this method approximates their values at time $\tau + \Delta\tau$ by a fourth-order polynominal in $\Delta\tau$.

The harmonic limit of Eq. (4.4) occurs as A_m tends to zero. When $A_m = 0.0001$, good agreement with the harmonic case was obtained. The interested reader can obtain more details on the program from the above reference 13.

The remainder of this paper will discuss the results of the numerical solution of Eq. (4.4) for different cases.

5. PROPAGATION IN THE INITIALLY QUIESCENT, ANHARMONIC LATTICE

In this section we will discuss the numerical solution of Eq. (4.4) for various values of the anharmonicity parameter A_m and rise time τ_{max}. For this discussion the following definitions are needed. The term solitary wave means a localized traveling wave of constant shape and amplitude. In this report, the term soliton describes a nonlinear solitary wave which emerges from a collision with a similar pulse, retaining the same shape and speed it had initially. Finally, the term envelope soliton describes an envelope of constant speed imposed on a solitary wave train with its own carrier speed.

The results are divided into four parts, each of which represents a different boundary condition on the zeroth particle. When the zeroth particle travels at constant velocity, we observe a solitary wave train at the head of the velocity trajectories of individual particles and an oscillatory tail which persists in the long-time limit. A sinusoidal acceleration on the zeroth particle produces what may be an envelope soliton traveling much slower than the shock wave. The same behavior is observed for a ramp acceleration. Finally, when the zeroth particle is decelerated to zero, an example of solitons spreading out in time is observed.

27. B. Carnahan, H.A. Luther, and J.O. Wilkes, Applied Numerical Methods (Wiley, New York, 1969), Chap. 6.

5.1 Zeroth Particle Travels at Constant Velocity

Let us look at the results of solving Eq. (4.4) under the boundary condition Eq. (4.3a). This physically corresponds to the case where the zeroth particle is pushed at constant speed for all time. For the anharmonicity parameter A_m=0.2, τ_{max}=0, and $\Delta\tau$=0.05 the velocity and position of selected particles is plotted as a function of tau. As the wave travels from the 10^{th} particle to the 90^{th} particle in Figure 11 to Figure 14, we see the amplitudes of the successive velocity peaks near the head of the shock wave gradually develop into a solitary wave train as was pointed out by Tasi[9] and Powell and Batteh[13]. The latter[13] have plotted the maximum particle velocity behind the shock front for A_m=0.2 and A_m=1.0 at a time when the front is approximately located at the 480^{th} particle. Their result indicates that the amplitudes of the leading solitary waves approach a dimensionless velocity of 2.0. The leading amplitudes for the case A_m=1.0 approace the value of 2.0 much sooner than the case A_m=0.2. The oscillatory tail is evident in Figure 11 and Figure 12 as was noticed by Tasi[7]. A similar oscillatory tail was reported by Zabusky in his numerical solution to the Korteweg-de Vries equation[28].

For the anharmonicity parameter A_m=1.0, τ_{max}=0.0, $\Delta\tau$=0.025, and boundary condition Eq. (4.3a), we see that the solitary wave train at the head of the shock wave has nearly formed at the 20^{th} particle in Figure 15. As the wave passes the 80^{th} and 240^{th} particle in Figure 16 and Figure 17 we notice that the leading amplitudes of successive velocity peaks have increased slightly over the 20^{th} particle. For all these cases we notice that the amplitudes of the oscillatory tail at times long after the shock has passed has not approached zero as was the case for the 10^{th} and 20^{th} particle for A_m=0.2. A careful examination of the 80^{th} and 240^{th} velocity trajectories will also show a slight spreading of the leading solitary waves. The greater the amplitude the faster they travel. This property is a characteristic of solitons. It was decided to observe the oscillatory tail at times long after the shock wave has passed. The 1^{st} and 5^{th} particles were observed for times greater than 200 in Figure 18 and Figure 19. The maximum amplitude of the 1^{st} particle is approximately 1.2 while that of the 5^{th} particle is approximately 1.5. The oscillatory tail for the 20^{th} particle

28. N.J. Zabusky, "Solitons and Bound States of the Time-Independent Schrodinger Equation", Phys. Rev. 168, 124 (1968).

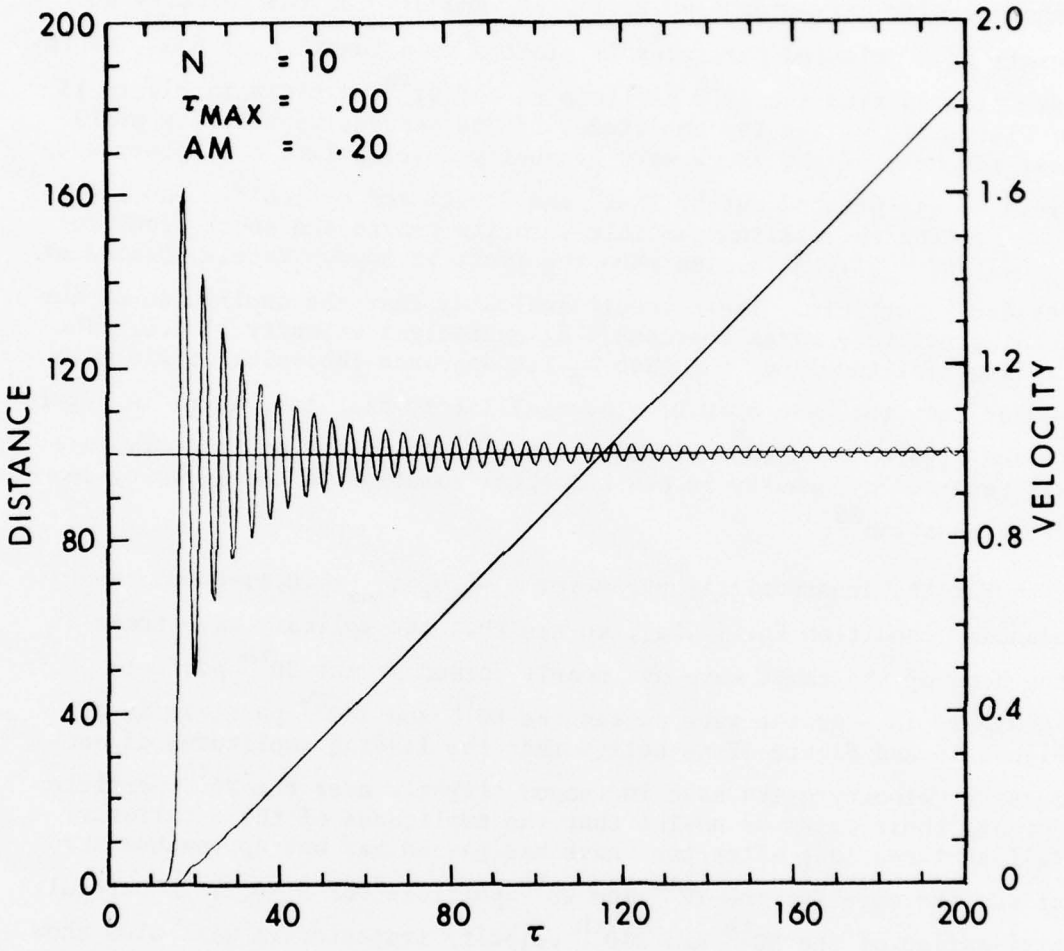

Figure 11. In dimensionless units the velocity which oscillates about unity and the displacement from equilibrium of the 10^{th} particle are plotted as a function of time for a lattice with an anharmonicity parameter A_m=.2 and a rise time τ_{max}=0.0.

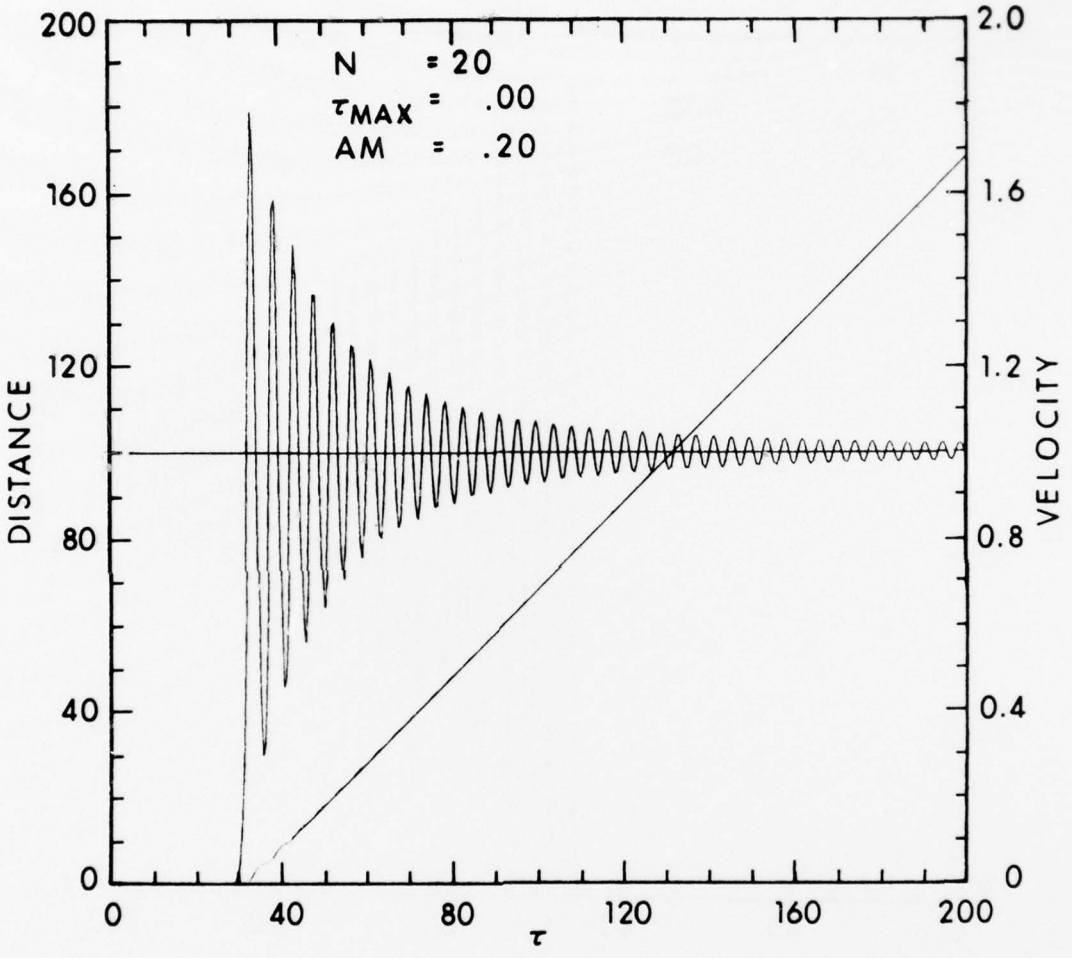

Figure 12. In dimensionless units the velocity which oscillates about unity and the displacement from equilibrium of the 20^{th} particle are plotted as a function of time for a lattice with an anharmonicity parameter A_m=.2 and a rise time τ_{max}=0.0.

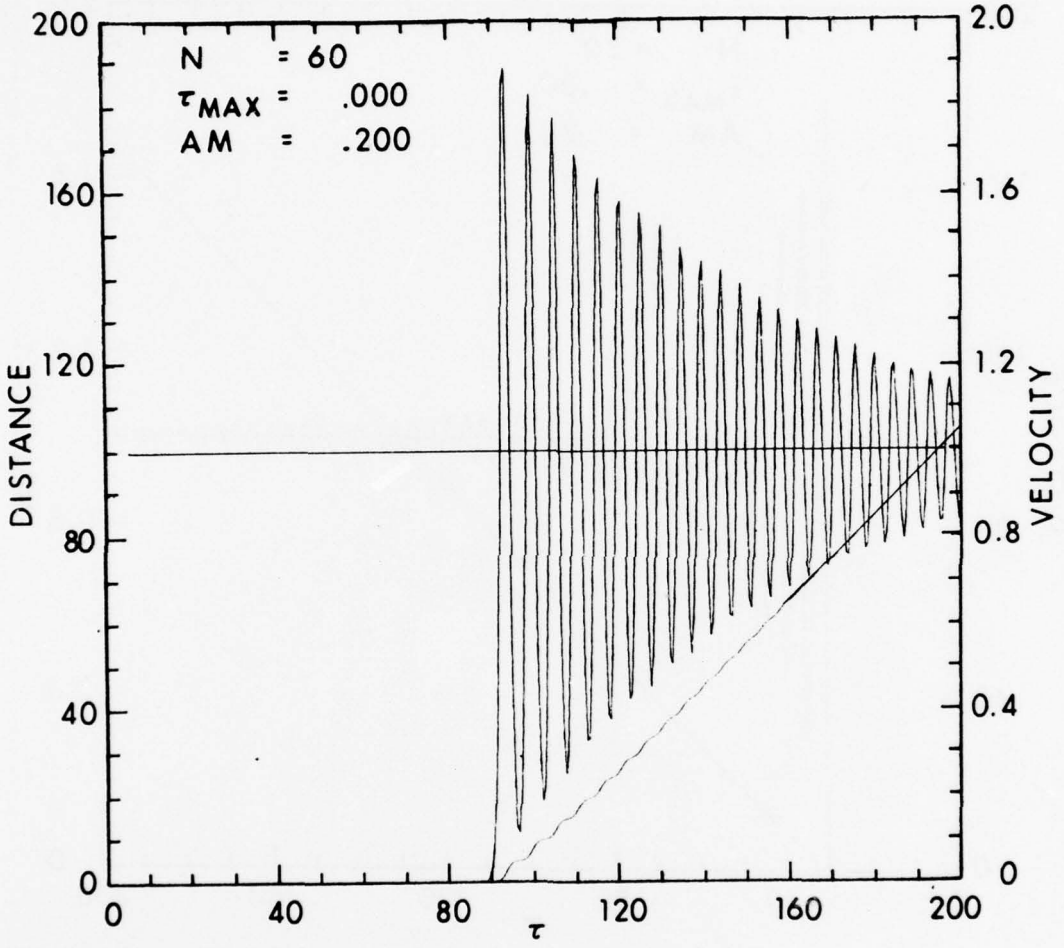

Figure 13. In dimensionless units the velocity which oscillates about unity and the displacement from equilibrium of the 60th particle are plotted as a function of time for a lattice with an anharmonicity parameter A_m=.2 and a rise time τ_{max}=0.0.

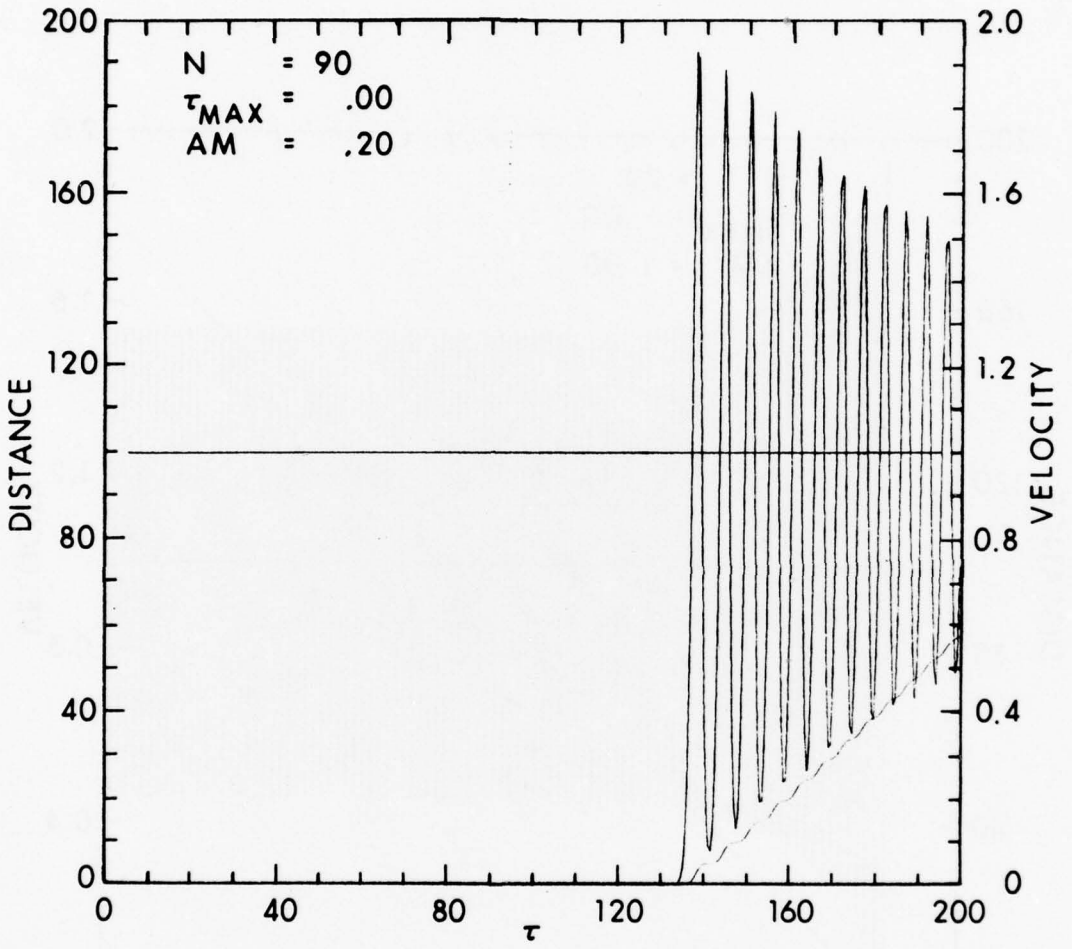

Figure 14. In dimensionless units the velocity which oscillates about unity and the displacement from equilibrium of the 90^{th} particle are plotted as a function of time for a lattice with an anharmonicity parameter A_m=.2 and a rise time τ_{max}=0.0.

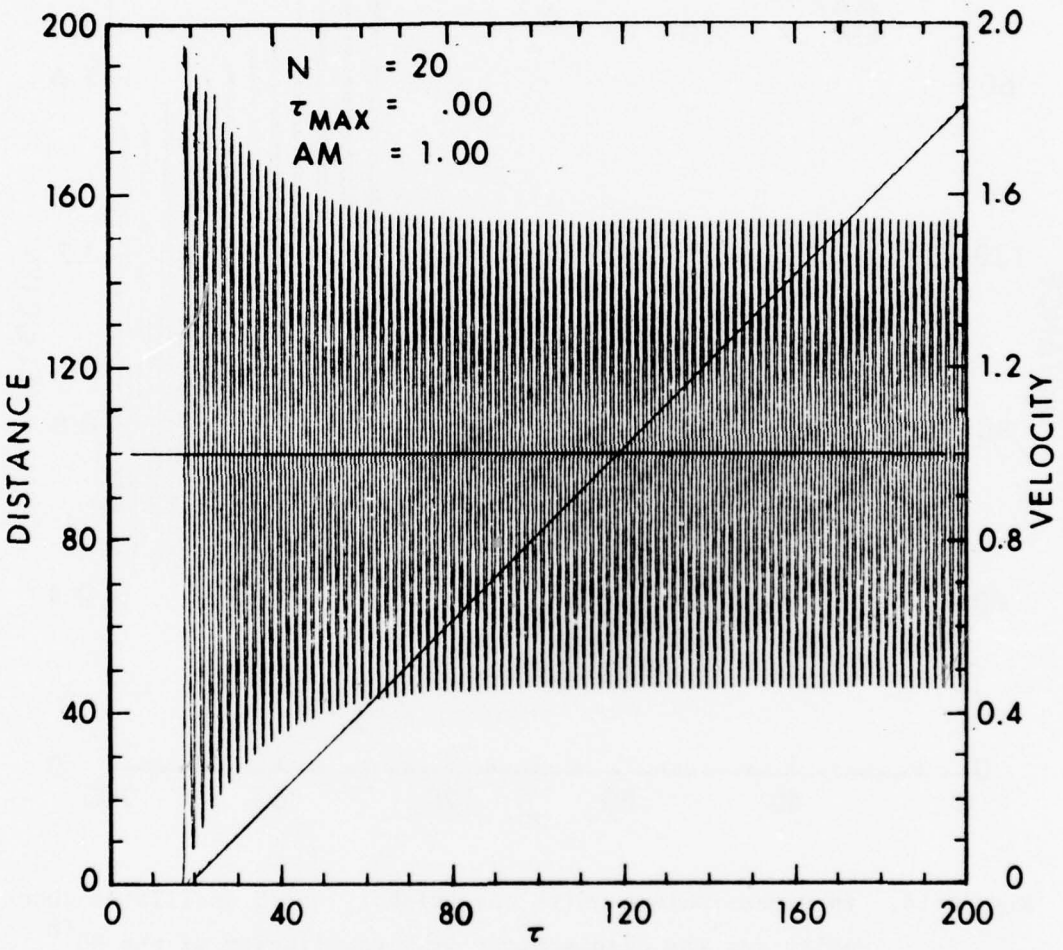

Figure 15. In dimensionless units the velocity which oscillates about unity and the displacement from equilibrium of the 20^{th} particle are plotted as a function of time for a lattice with an anharmonicity parameter A_m=1.0 and a rise time τ_{max}=0.0.

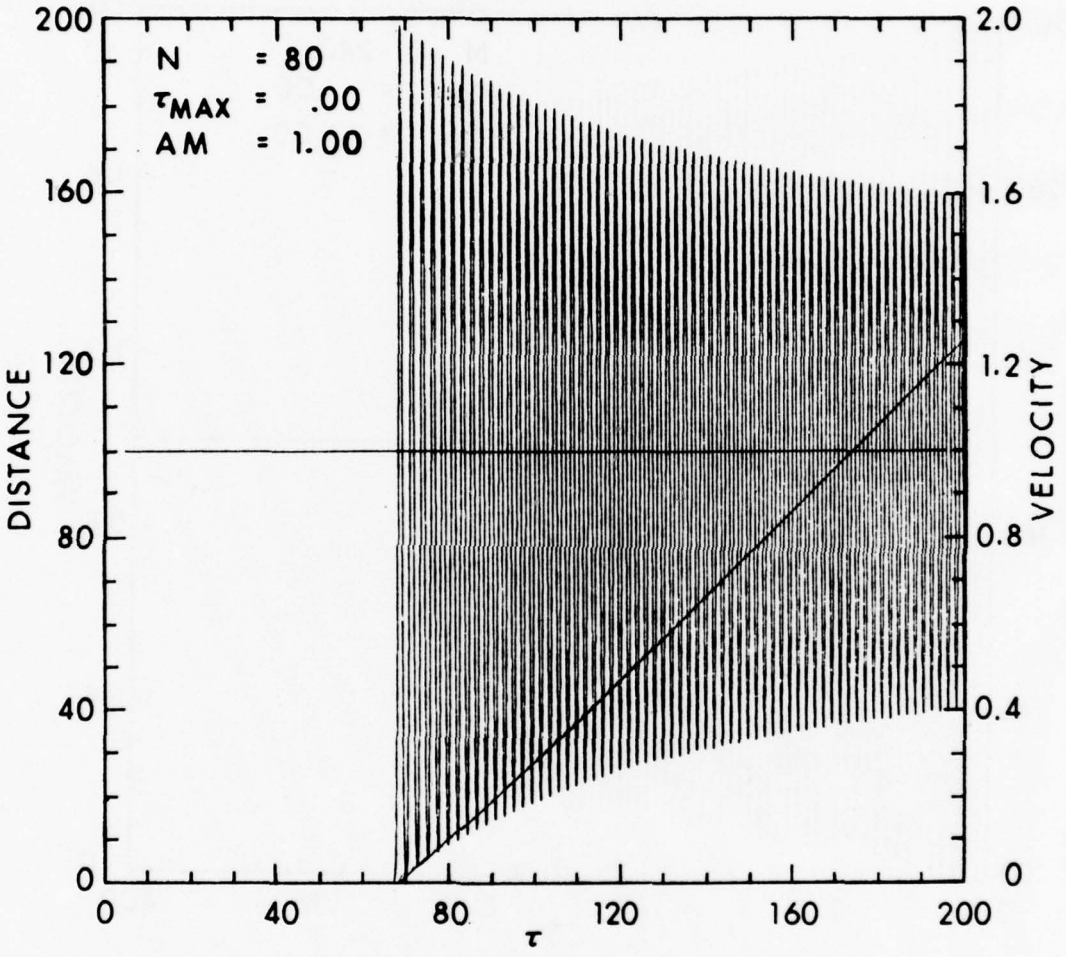

Figure 16. In dimensionless units the velocity which oscillates about unity and the displacement from equilibrium of the 80^{th} particle are plotted as a function of time for a lattice with an anharmonicity parameter A_m=1.0 and a rise time τ_{max}=0.0.

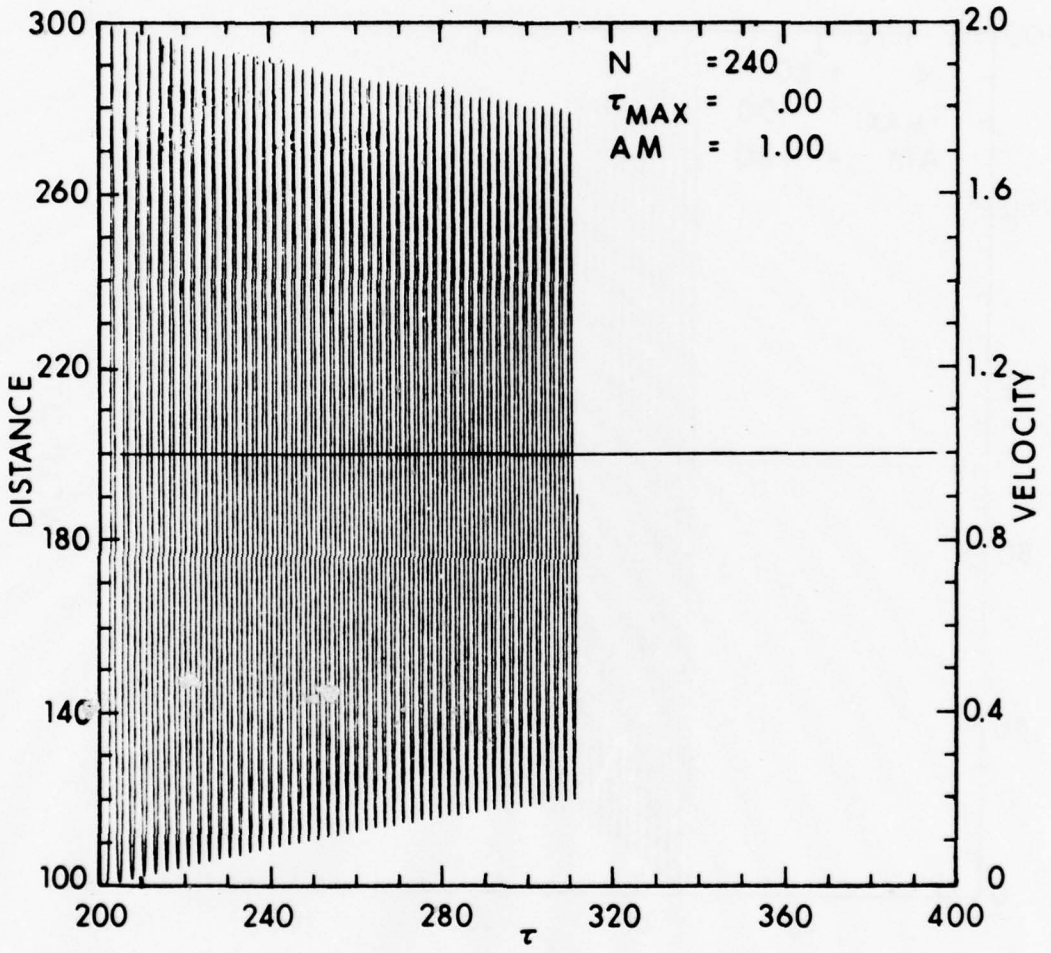

Figure 17. In dimensionless units the velocity which oscillates about unity and the displacement from equilibrium of the 240th particle are plotted as a function of time for a lattice with an anharmonicity parameter A_m=1.0 and a rise time τ_{max}=0.0.

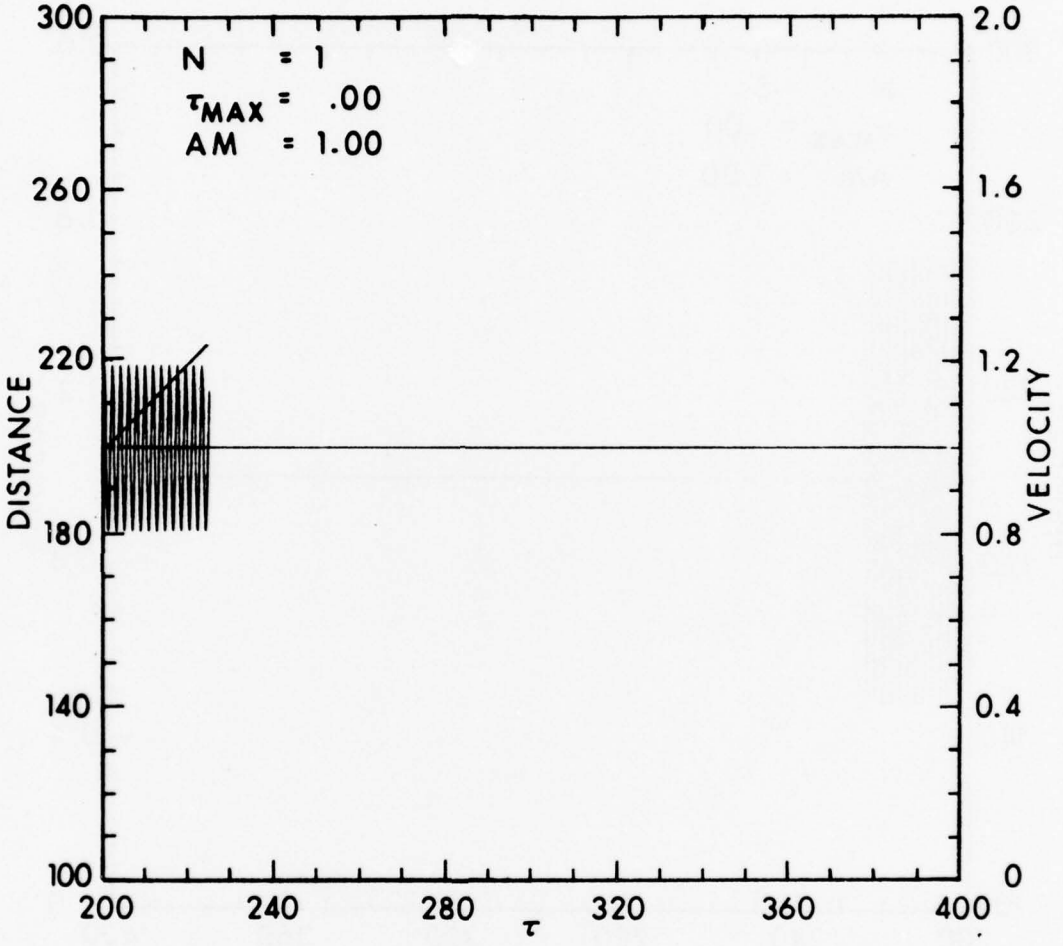

Figure 18. In dimensionless units the velocity which oscillates about unity and the displacement from equilibrium of the 1st particle are plotted as a function of time for a lattice with an anharmonicity parameter A_m=1.0 and a rise time τ_{max}=0.0.

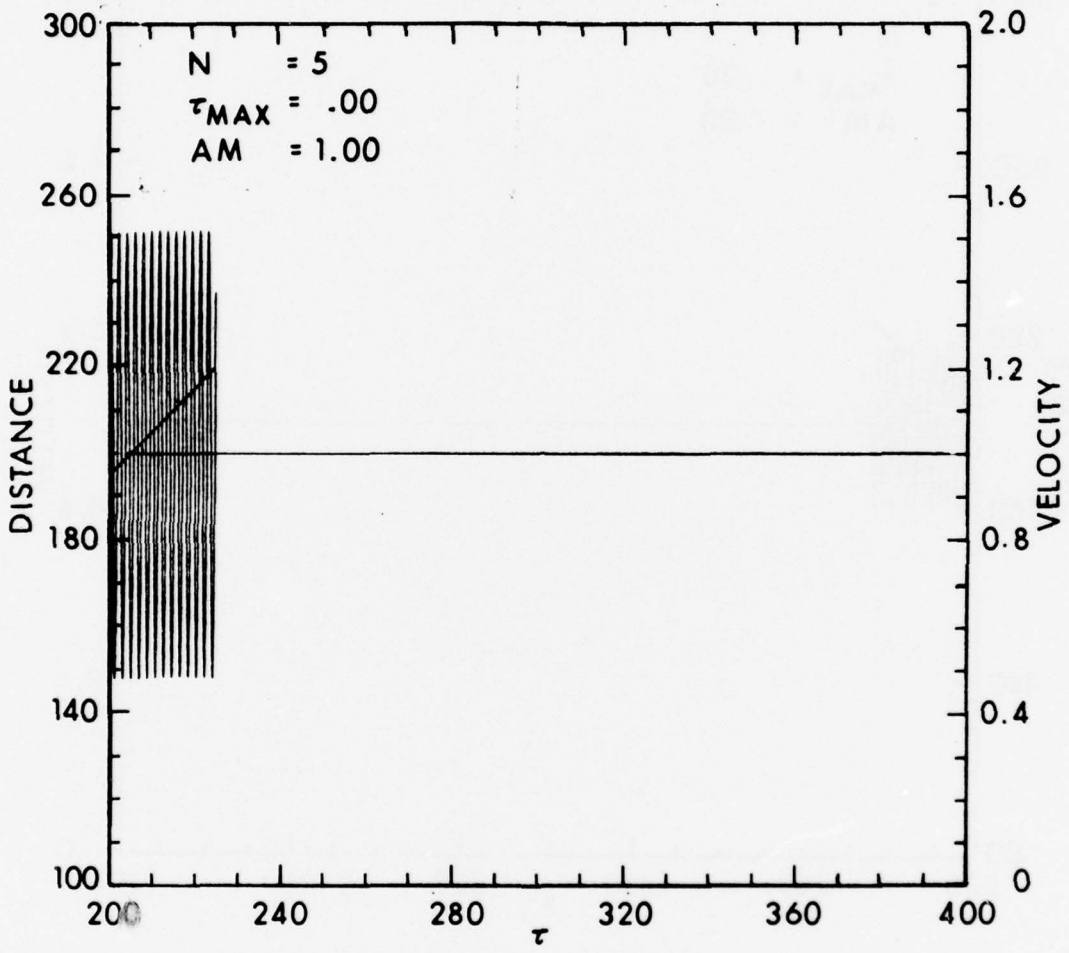

Figure 19. In dimensionless units the velocity which oscillates about unity and the displacement from equilibrium of the 5^{th} particle are plotted as a function of time for a lattice with an anharmonicity parameter A_m=1.0 and a rise time τ_{max}=0.0.

in Figure 20 was observed for a much longer period of time, and its maximum amplitude was found to be slightly greater than the 5^{th} particle.

5.2 Zeroth Particle Accelerated Sinusoidally

Let us compare the results of solving Eq. (4.4) under the boundary condition Eq. (4.3b) to the ones obtained under the boundary condition Eq. (4.3a). This physically corresponds to the case where the zeroth particle is accelerated sinusoidally from zero velocity to its final velocity in time τ_{max}. For the anharmonicity parameter A_m=0.2, τ_{max}=12.0, and $\Delta\tau$=0.5, we observe that the amplitude of the velocity of the shock wave at the 20^{th} particle in Figure 21 is less than the case τ_{max}=0.0 in Figure 12. As the shock wave reaches the 60^{th} particle the leading peak in Figure 22 is the same as Figure 13, but the succeeding pulses are less in amplitude. According to our results, by the time the wave has reached the 80^{th} particle, the cases τ_{max}=0.0 and τ_{max}=12.0 look the same. Therefore, for a low anharmonicity parameter such as A_m=0.2 each amplitude of the successive peaks in the wave train for surface particles is less than the corresponding amplitude for the instantaneous compression case by an amount which is inversely proportional to the rise time τ_{max}. This phenomenon is analogous to the harmonic case. The most distinguishing factor between the harmonic and slightly anharmonic cases is the steeper and narrower pulse width for the latter, which gradually develops into a solitary wave train.

For the anharmonicity parameter A_m=1.0, τ_{max}=12.0 and $\Delta\tau$=.025 not only do we see the characteristics already described at lower anharmonicities, but also the appearance of a dip in the amplitude of the velocity at a time after the shock wave has passed an individual particle. Perhaps, the disturbance is an envelope soliton. In Figure 23 to Figure 27 we observe the envelope traveling past the 20^{th}, 30^{th}, 40^{th}, and 60^{th} particle at approximately one sixth the speed of the shock front. The amount of computer time prevented us from following the envelope past 325 tau. The velocity trajectory of the 60^{th} particle has the same profile for τ_{max}=0 as for τ_{max}=12.0 except in the vicinity of the envelope from the time the shock wave arrives until 325 tau. The profiles of particles greater than 60 look alike up to 325 tau as the envelope would be expected to appear at a later time. In Figure 28 we show the initial solitary waves arriving at the 380^{th} particle for the case τ_{max}=12.0, but we expect the same initial profile to hold for other values of τ_{max}. The 380^{th} particle is the farthest point in the lattice for which we were able to compute a meaningful profile.

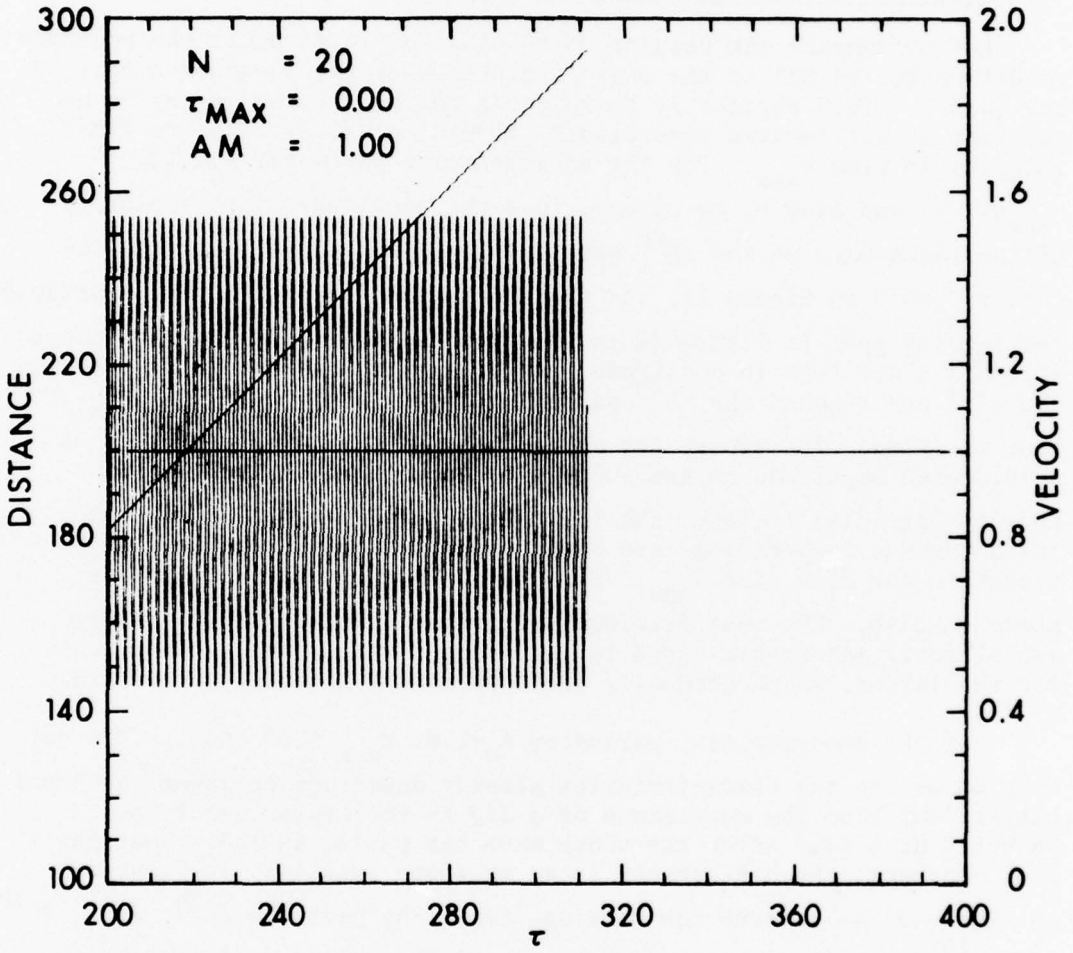

Figure 20. In dimensionless units the velocity which oscillates about unity and the displacement from equilibrium of the 20^{th} particle are plotted as a function of time for a lattice with an anharmonicity parameter A_m=1.0 and a rise time τ_{max}=0.0.

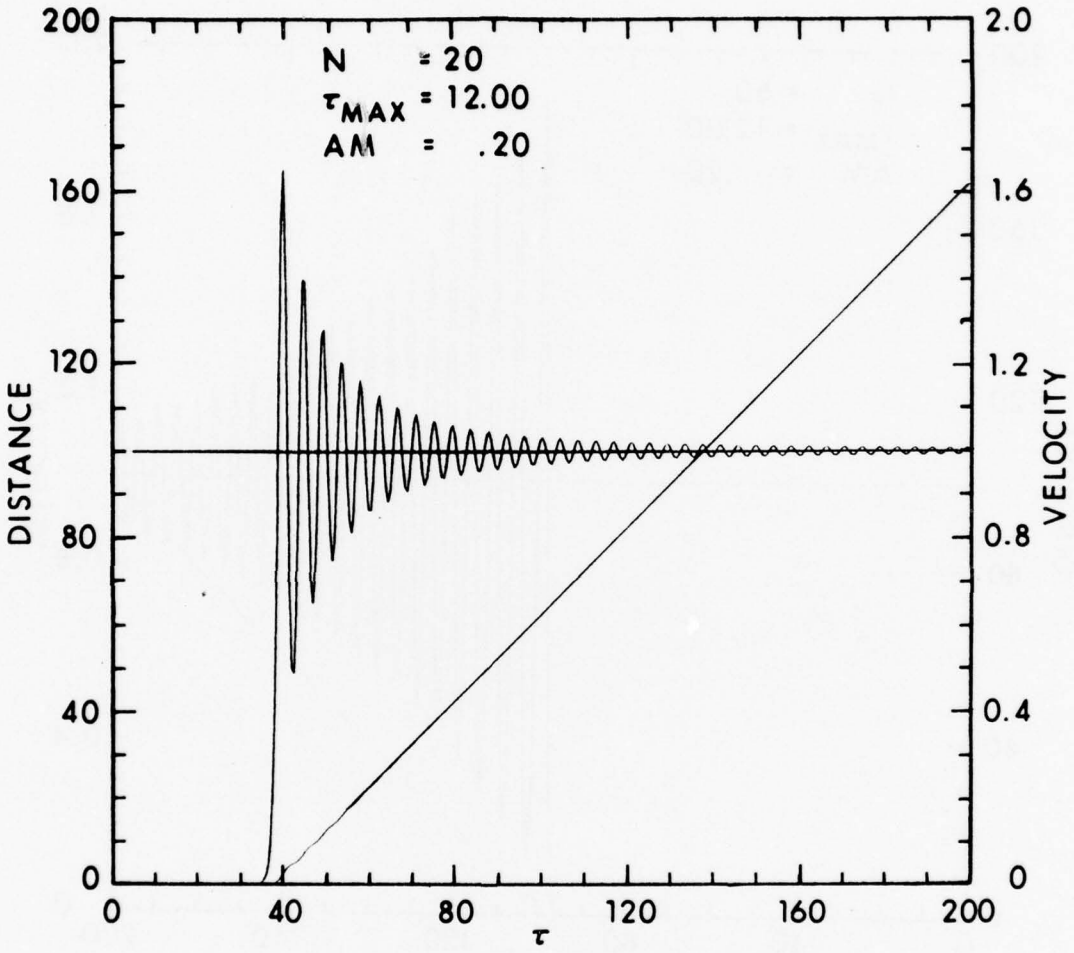

Figure 21. In dimensionless units the velocity which oscillates about unity and the displacement from equilibrium of the 20^{th} particle are plotted as a function of time for a lattice with an anharmonicity parameter A_m=.2 and a rise time τ_{max}=12.0.

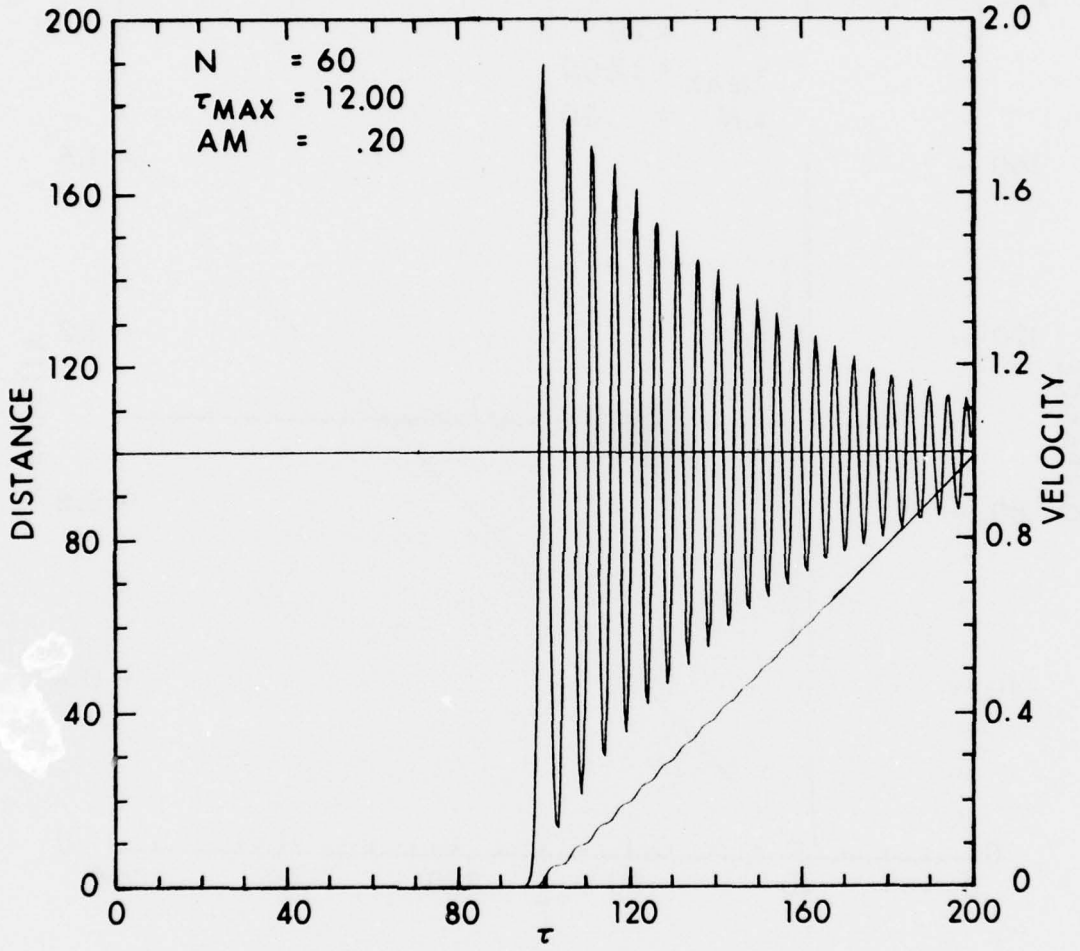

Figure 22. In dimensionless units the velocity which oscillates about unity and the displacement from equilibrium of the 60^{th} particle are plotted as a function of time for a lattice with an anharmonicity parameter A_m=.2 and a rise time τ_{max}=12.0.

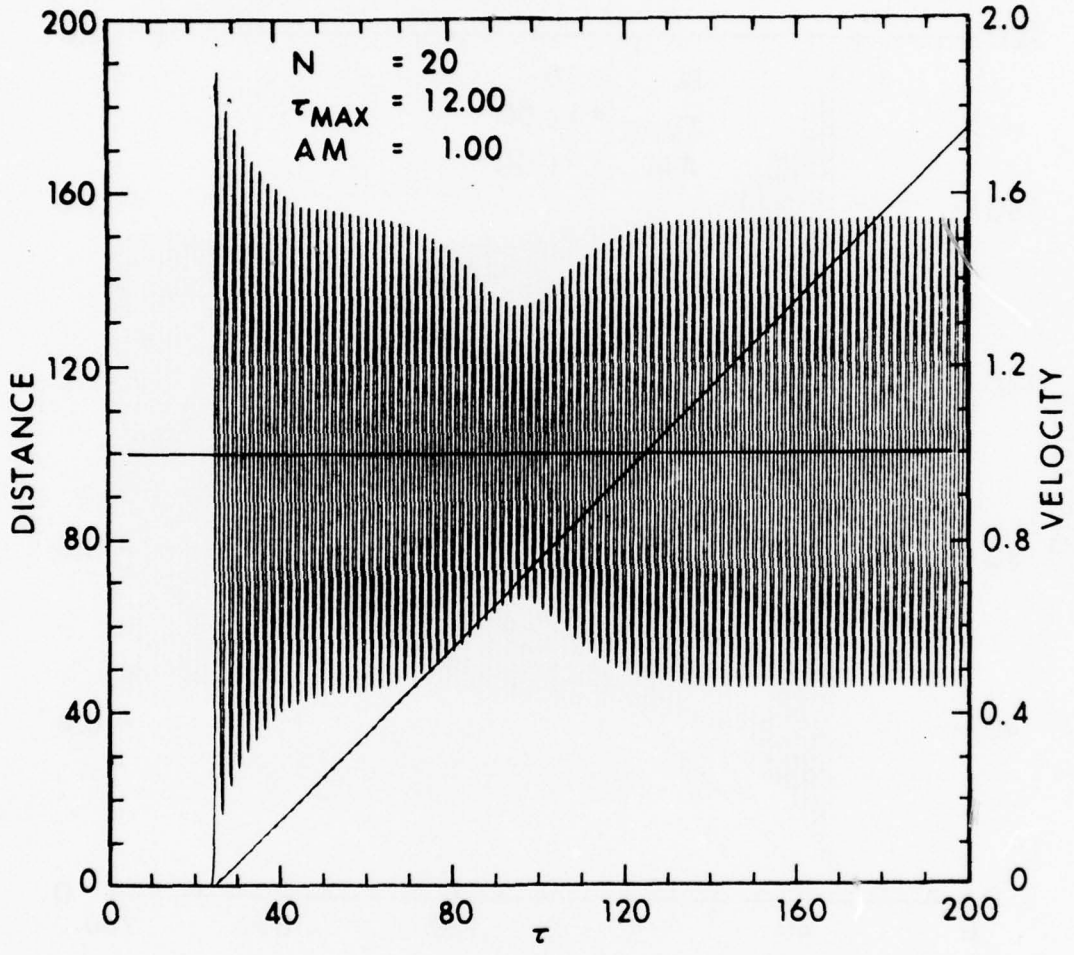

Figure 23. In dimensionless units the velocity which oscillates about unity and the displacement from equilibrium of the 20^{th} particle are plotted as a function of time for a lattice with an anharmonicity parameter A_m=1.0 and a rise time τ_{max}=12.0.

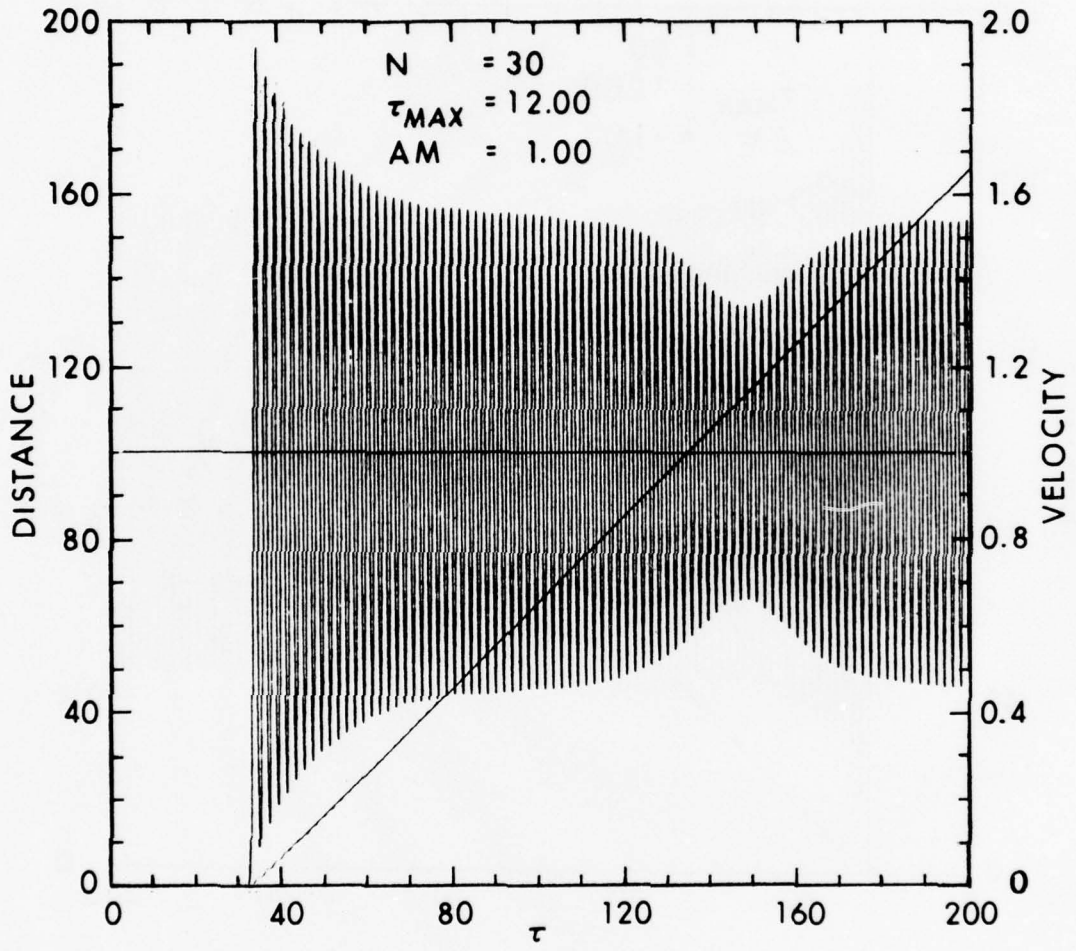

Figure 24. In dimensionless units the velocity which oscillates about unity and the displacement from equilibrium of the 30^{th} particle are plotted as a function of time for a lattice with an anharmonicity parameter A_m=1.0 and a rise time τ_{max}=12.0.

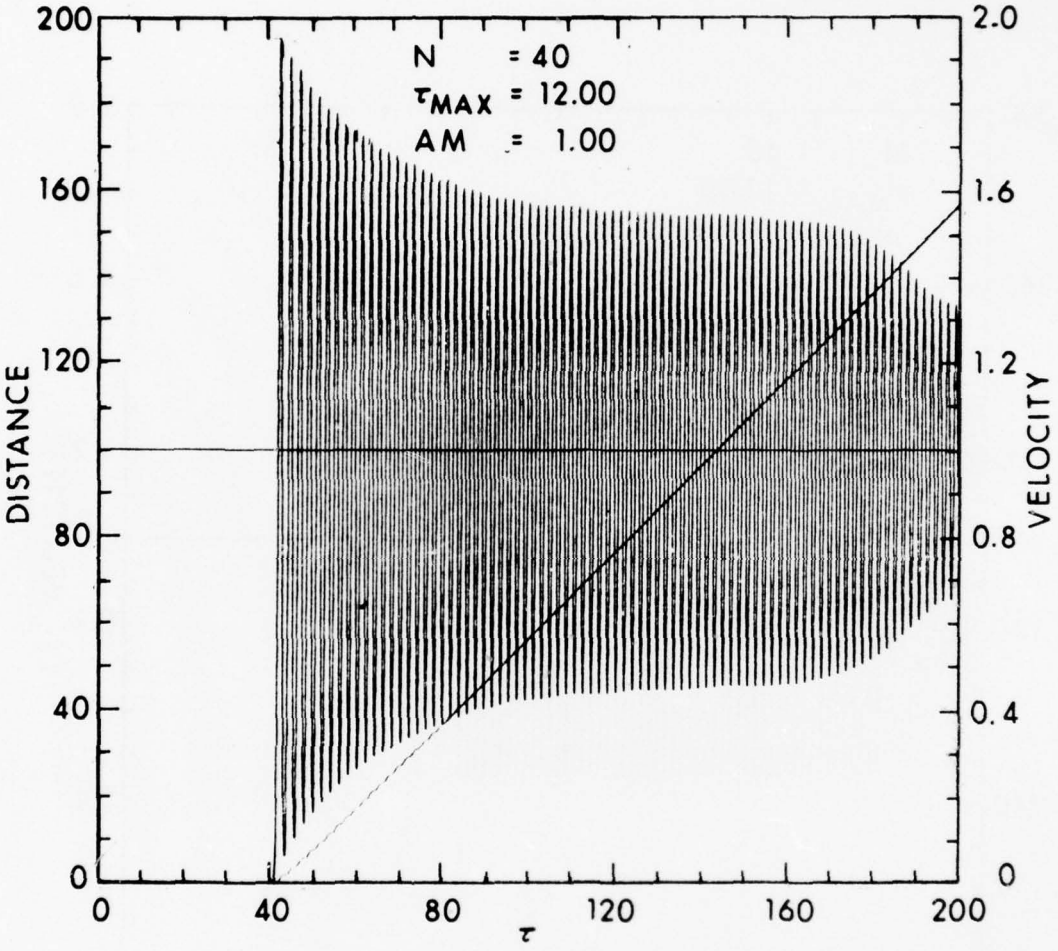

Figure 25. In dimensionless units the velocity which oscillates about unity and the displacement from equilibrium of the 40^{th} particle are plotted as a function of time for a lattice with anharmonicity parameter A_m=1.0 and a rise time τ_{max}=12.0.

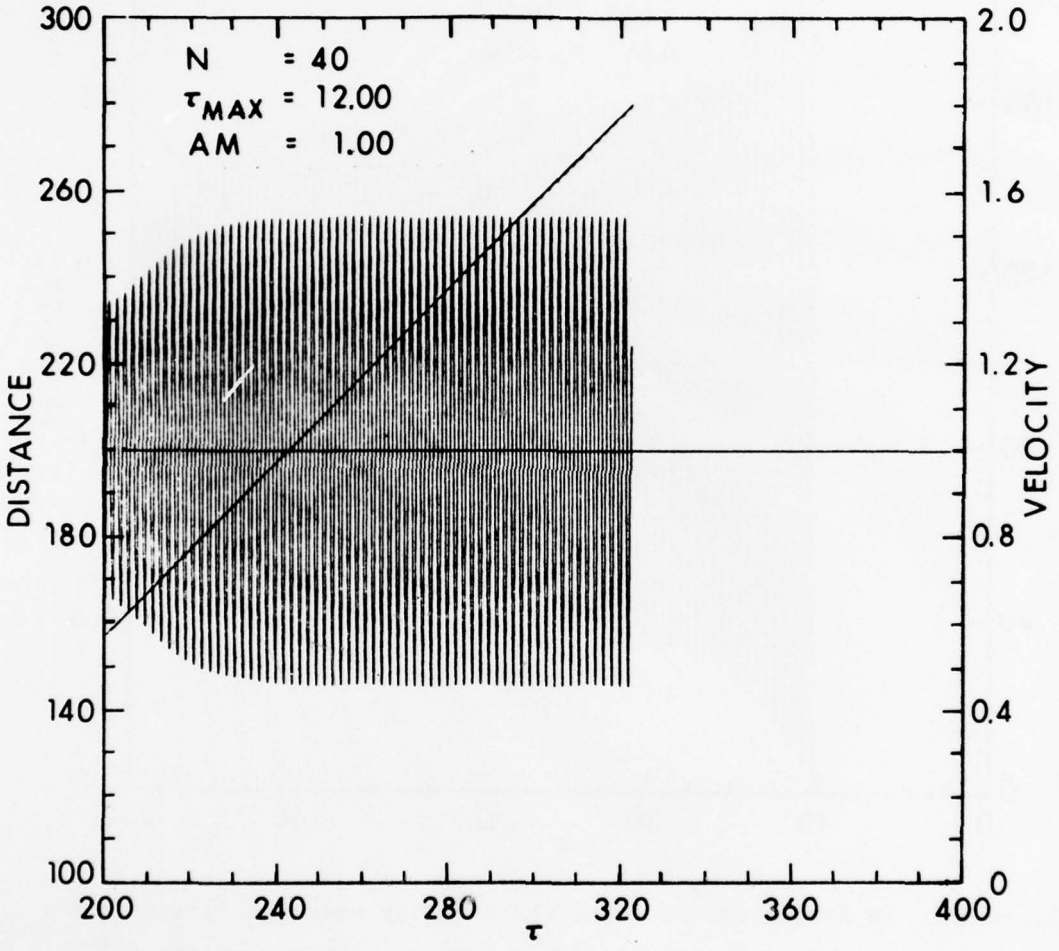

Figure 26. In dimensionless units the velocity which oscillates about unity and the displacement from equilibrium of the 40^{th} particle are plotted as a function of time for a lattice with an anharmonicity parameter A_m=1.0 and rise time τ_{max}=12.0.

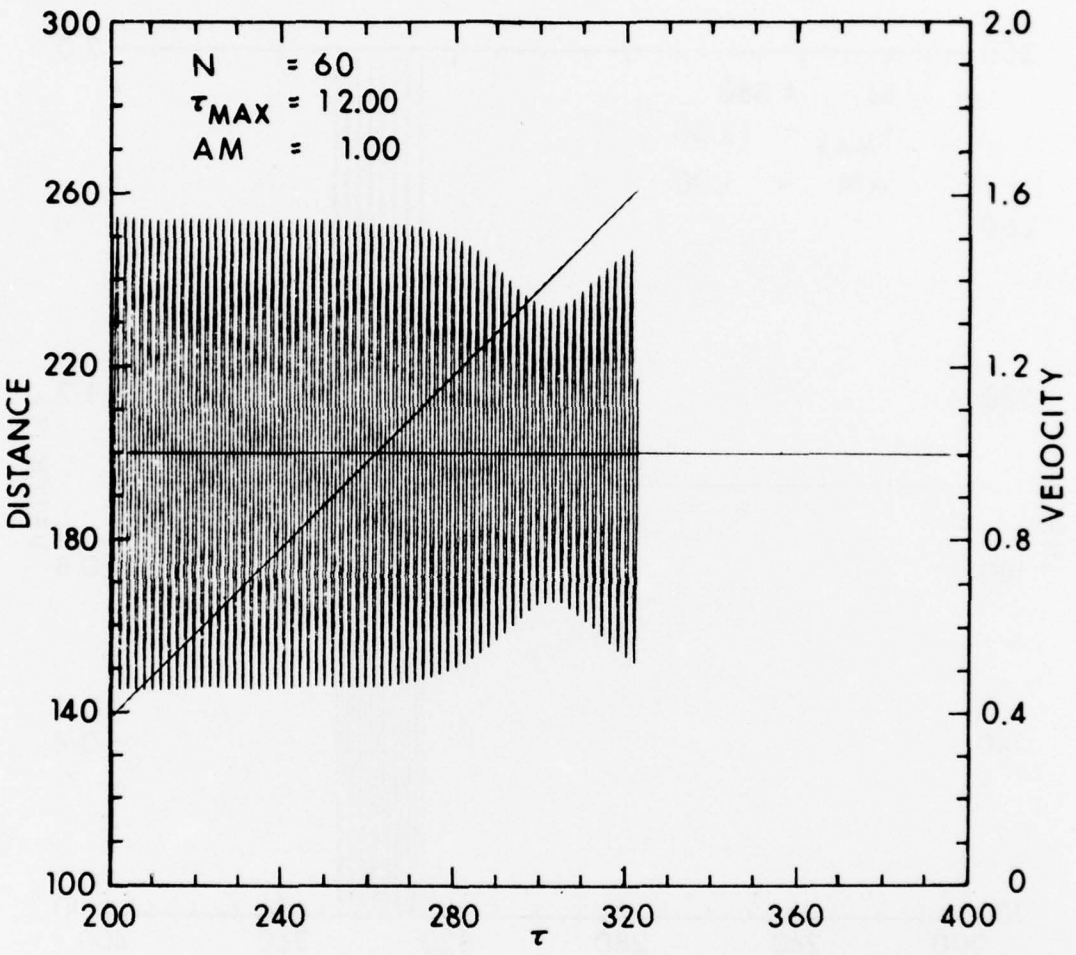

Figure 27. In dimensionless units the velocity which oscillates about unity and the displacement from equilibrium of the 60th particle are plotted as a function of time for a lattice with an anharmonicity parameter $A_{\bar{m}}$=1.0 and rise time τ_{max}=12.0.

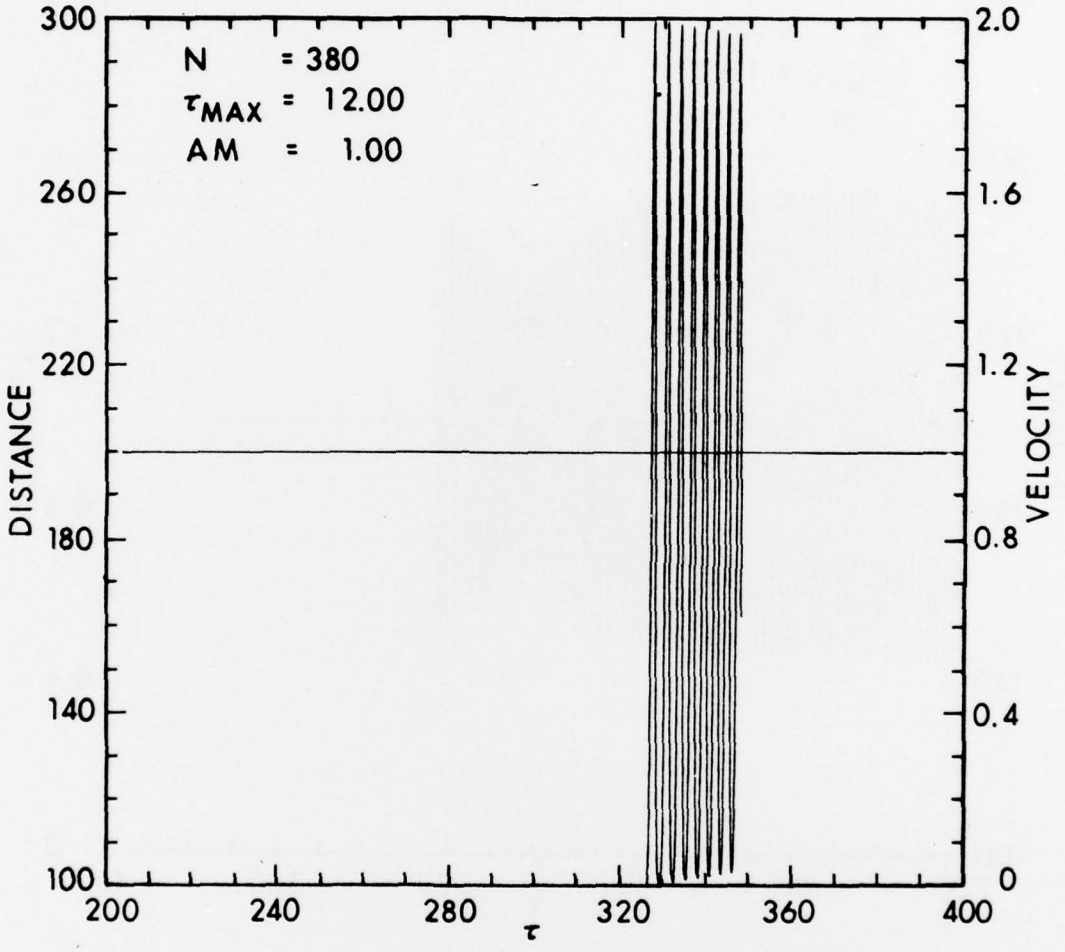

Figure 28. In dimensionless units the velocity of the 380th particle which oscillates about unity is plotted as a function of time for a lattice with an anharmonicity parameter A_m=1.0 and rise time τ_{max}=12.0.

We wanted to verify that the envelope would occur for other anharmonicities, and at the same time investigate the effect of different rise times τ_{max}. For the anharmonicity parameter A_m=1.2, and $\Delta\tau$=0.025 we looked at the ninth particle for different values of τ_{max}. For τ_{max}=4.0 we see no envelope at all in Figure 29. This result is most likely explained by the fact that as τ_{max} approaches zero no envelope has been reported by any investigator. For values of τ_{max}=8.0, 12.0, and 20.0 in Figure 30 through Figure 32, respectively, we observe an envelope which appears to deepen and appear at a later time relative to the arrival of the initial disturbance at the ninth particle.

5.3 Zeroth Particle Given a Ramp Acceleration

We wanted to make sure that what seemed to be an envelope soliton was not caused by our choice of the sinusoidal acceleration given to the zeroth particle, rather than some other acceleration, like the ramp acceleration in Eq. (4.3c). For the anharmonicity parameter A_m=1.2, and $\Delta\tau$=.025 an envelope was observed at the ninth particle for τ_{max}=4.0 and τ_{max}=12.0 in Figure 33 and Figure 34, respectively. Even for τ_{max}=4.0 an envelope was formed in contrast to the case in Figure 29 for the same rise time. For τ_{max}=12.0 the envelope was deeper than the case τ_{max}=4.0 and occurred at a later time after the arrival of the shock wave.

5.4 Zeroth Particle Decelerated to Zero

Finally, we wanted to see the effect of starting the zeroth particle at constant velocity and then decelerating it to zero in time τ_{max}. The boundary condition is Eq. (4.3a) minus Eq. (4.3b). For the anharmonicity parameter A_m=1.0, $\Delta\tau$=.025, and τ_{max}=12.0 we have a beautiful example of solitons spreading out in time starting at the tenth particle in Figure 35 and going to the fortieth particle in Figure 36.

6. DISCUSSION

In this report we have investigated the effect of accelerating the end particle of a one-dimensional lattice to its final velocity in a characteristic time τ_{max}. The purpose was to determine the shock profile caused in this manner and compare it with the instantaneous compression case. For harmonic lattices we noticed that in the surface atoms each amplitude of the successive peaks in the wave train was less

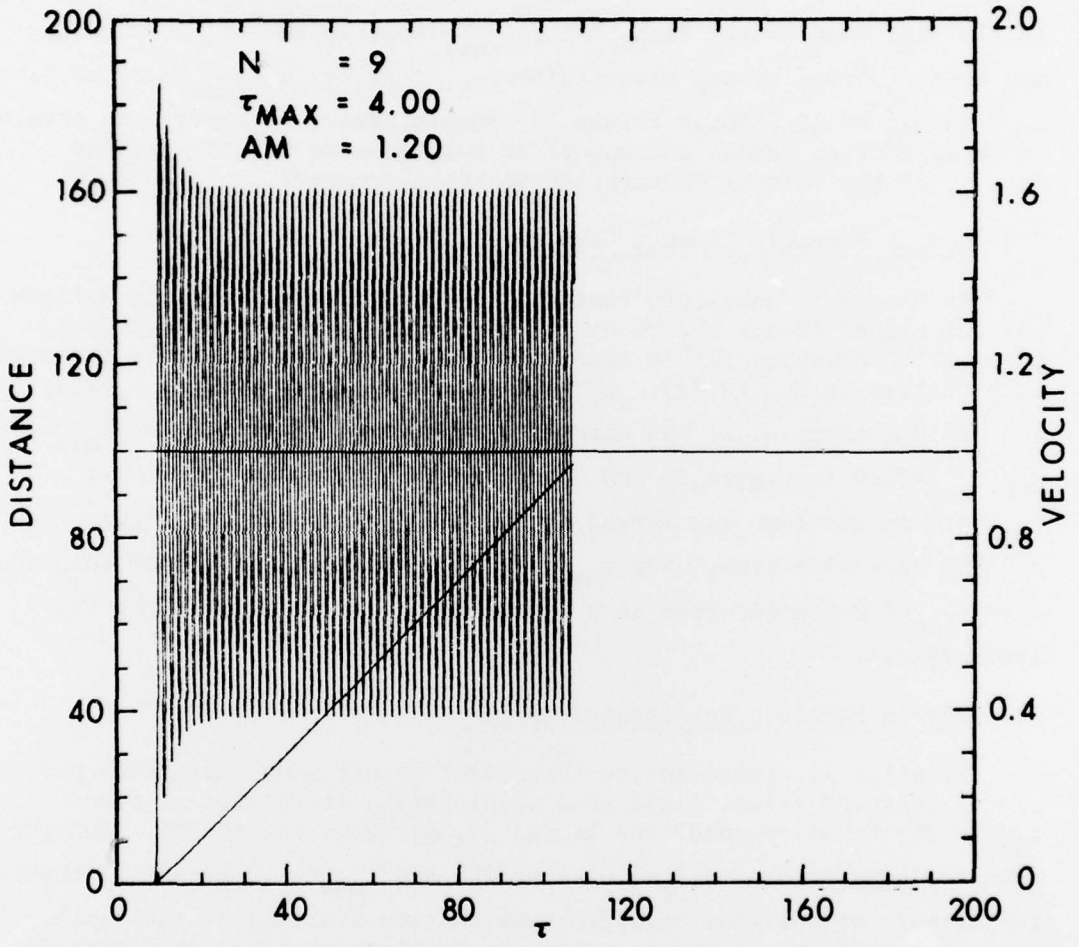

Figure 29. In dimensionless units the velocity which oscillates about unity and the displacement from equilibrium of the 9^{th} particle are plotted as a function of time for a lattice with an anharmonicity parameter A_m=1.2 and rise time τ_{max}=4.0.

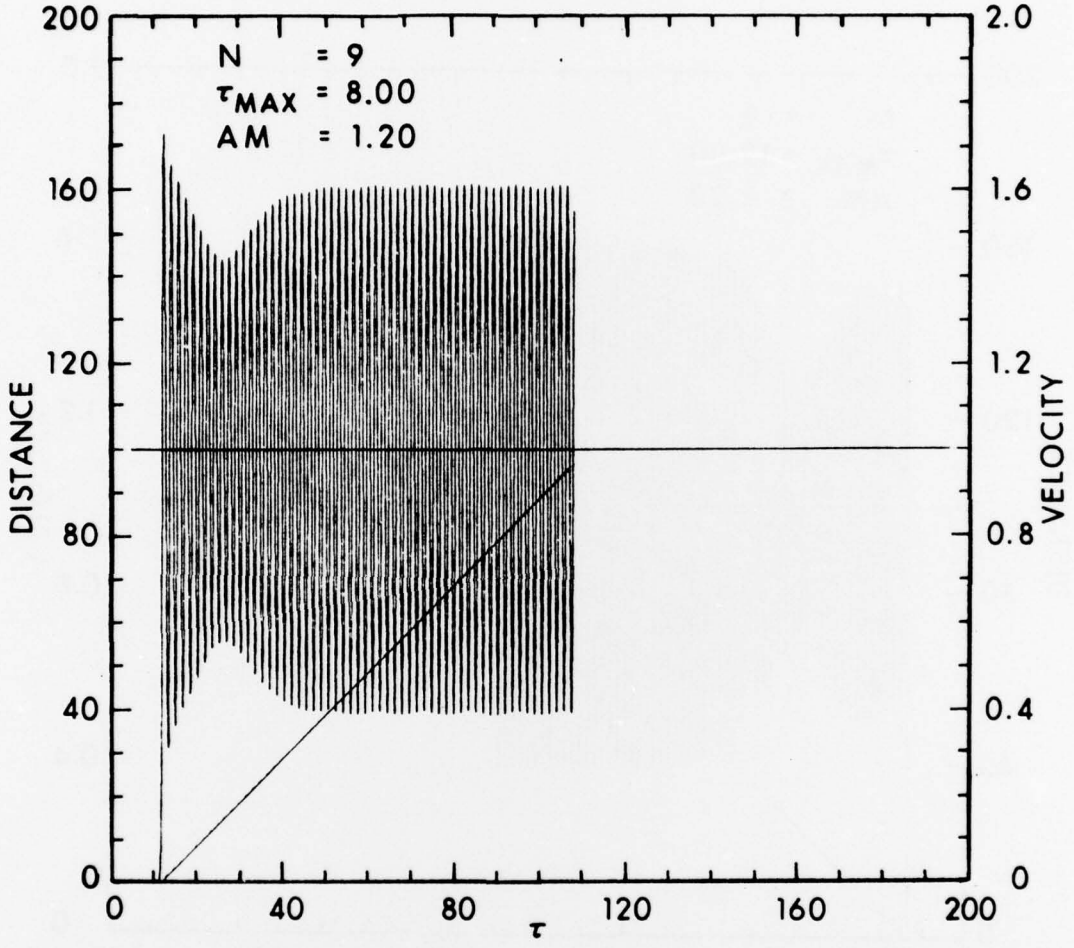

Figure 30. In dimensionless units the velocity which oscillates about unity and the displacement from equilibrium of the 9^{th} particle are plotted as a function of time for a lattice with an anharmonicity parameter A_m=1.2 and rise time τ_{max}=8.0.

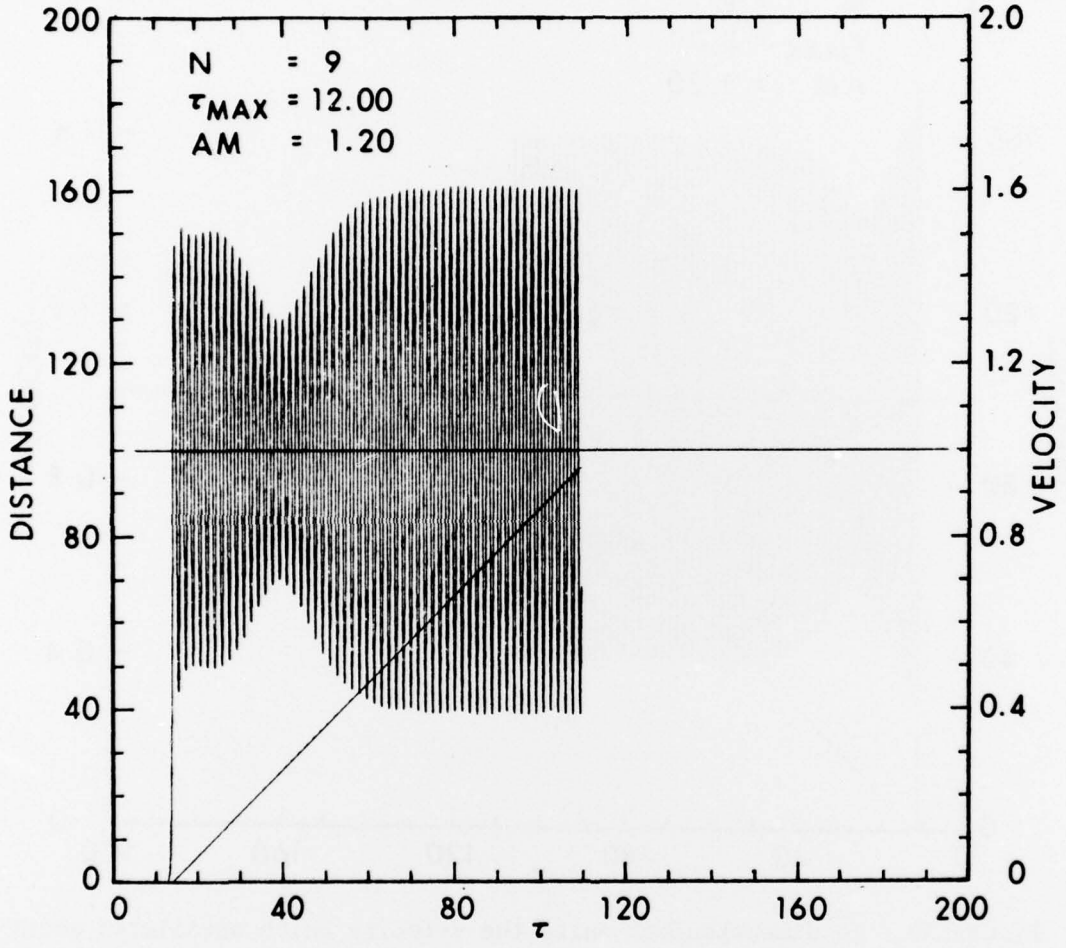

Figure 31. In dimensionless units the velocity which oscillates about unity and the displacement from equilibrium of the 9^{th} particle are plotted as a function of time for a lattice with an anharmonicity parameter A_m=1.2 and rise time τ_{max}=12.0.

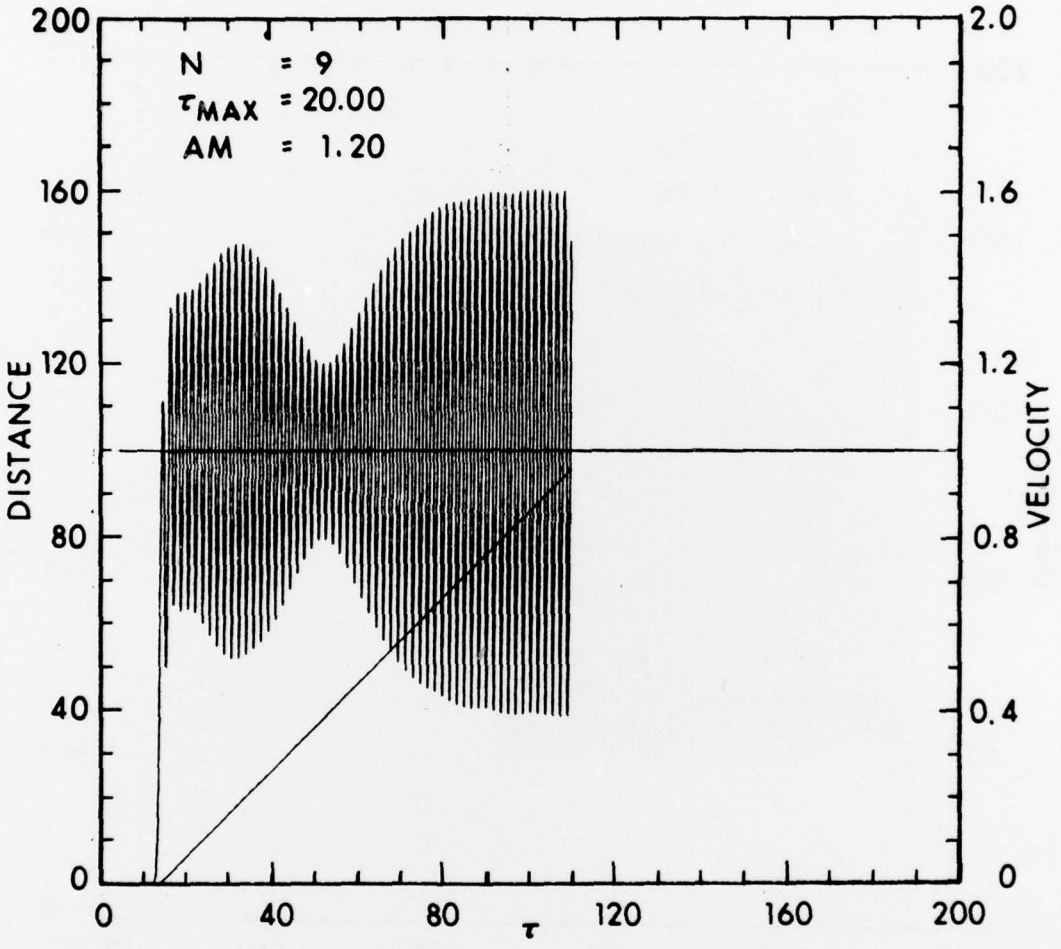

Figure 32. In dimensionless units the velocity which oscillates about unity and the displacement from equilibrium of the 9^{th} particle are plotted as a function of time for a lattice with an anharmonicity parameter A_m=1.2 and rise time τ_{max}=20.0.

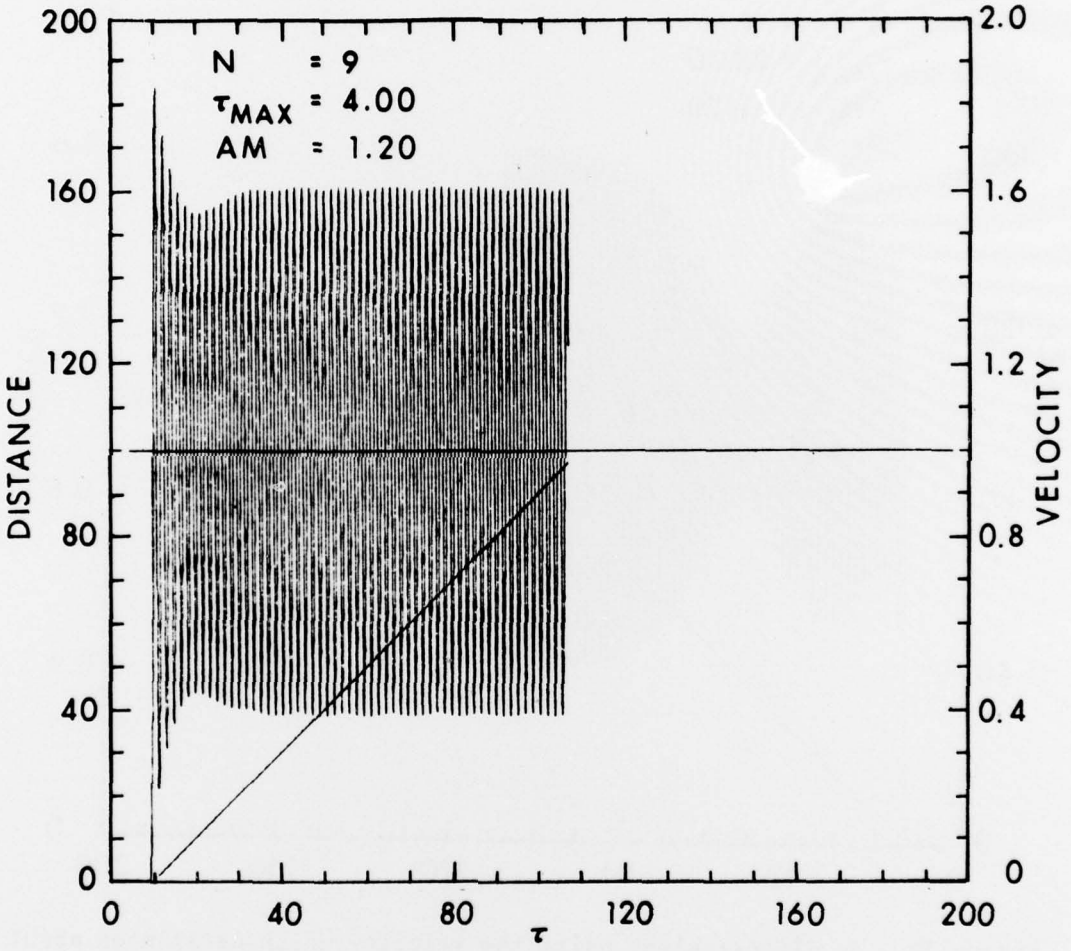

Figure 33. In dimensionless units the velocity which oscillates about unity and the displacement from equilibrium of the 9^{th} particle are plotted as a function of time for a lattice with an anharmonicity parameter A_m=1.2 and rise time τ_{max}=4.0. A ramp acceleration of zeroth particle is used.

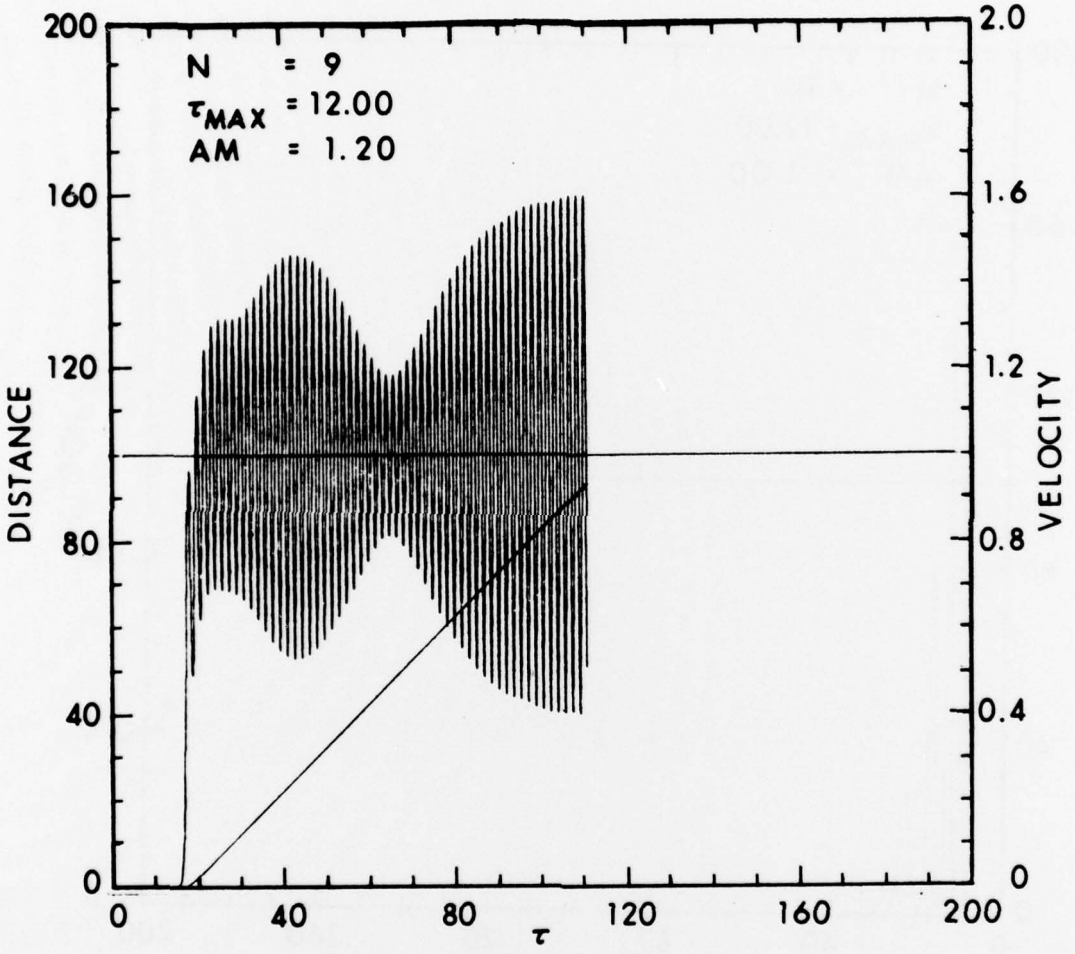

Figure 34. In dimensionless units the velocity which oscillates about unity and the displacement from equilibrium of the 9^{th} particle are plotted as a function of time for lattice with an anharmonicity parameter A_m=1.2 and rise time τ_{max}=12.0. A ramp acceleration of zeroth particle is used.

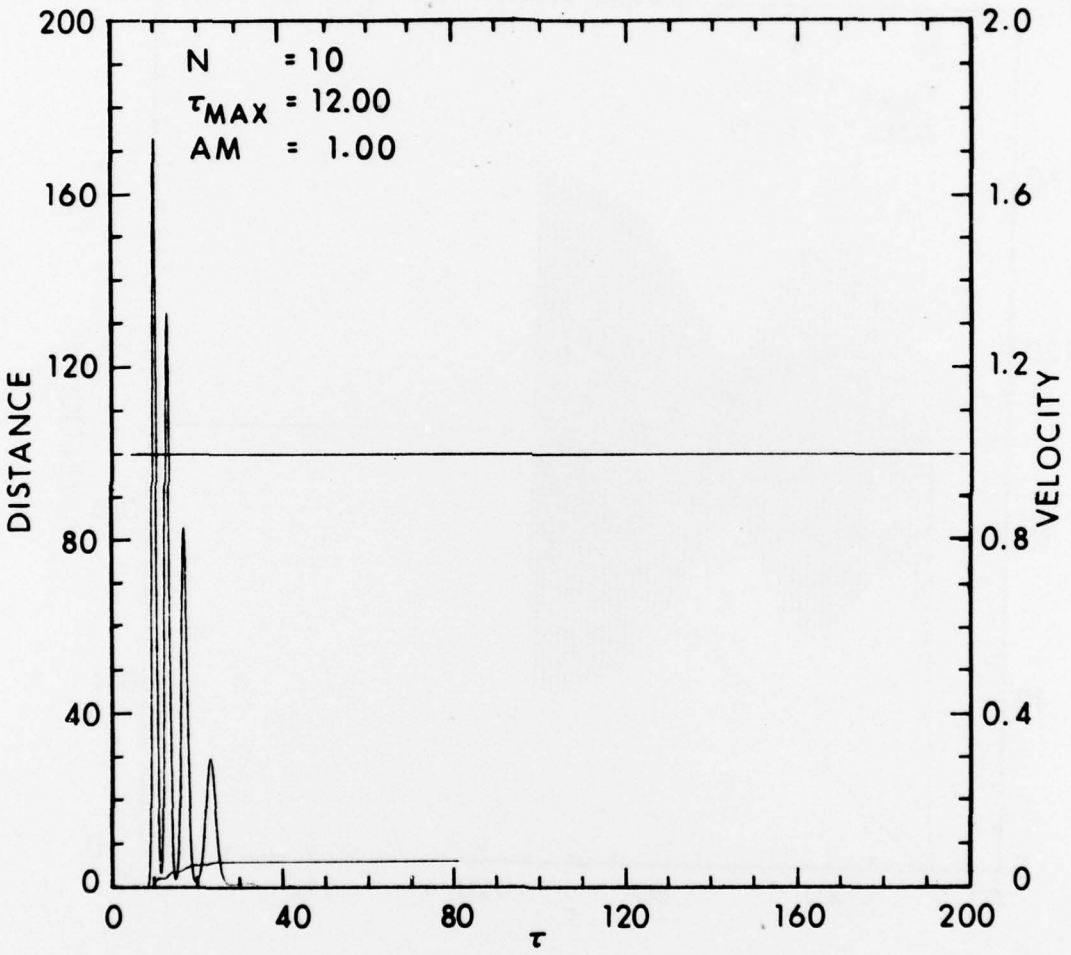

Figure 35. In dimensionless units the velocity which propagates as four solitary waves and the displacement from equilibrium of the 10^{th} particle are plotted as a function of time for a lattice with an anharmonicity parameter A_m=1.0 and deceleration time τ_{max}=12.0. The zeroth particle starts out with initial velocity of unity and is decelerated to zero.

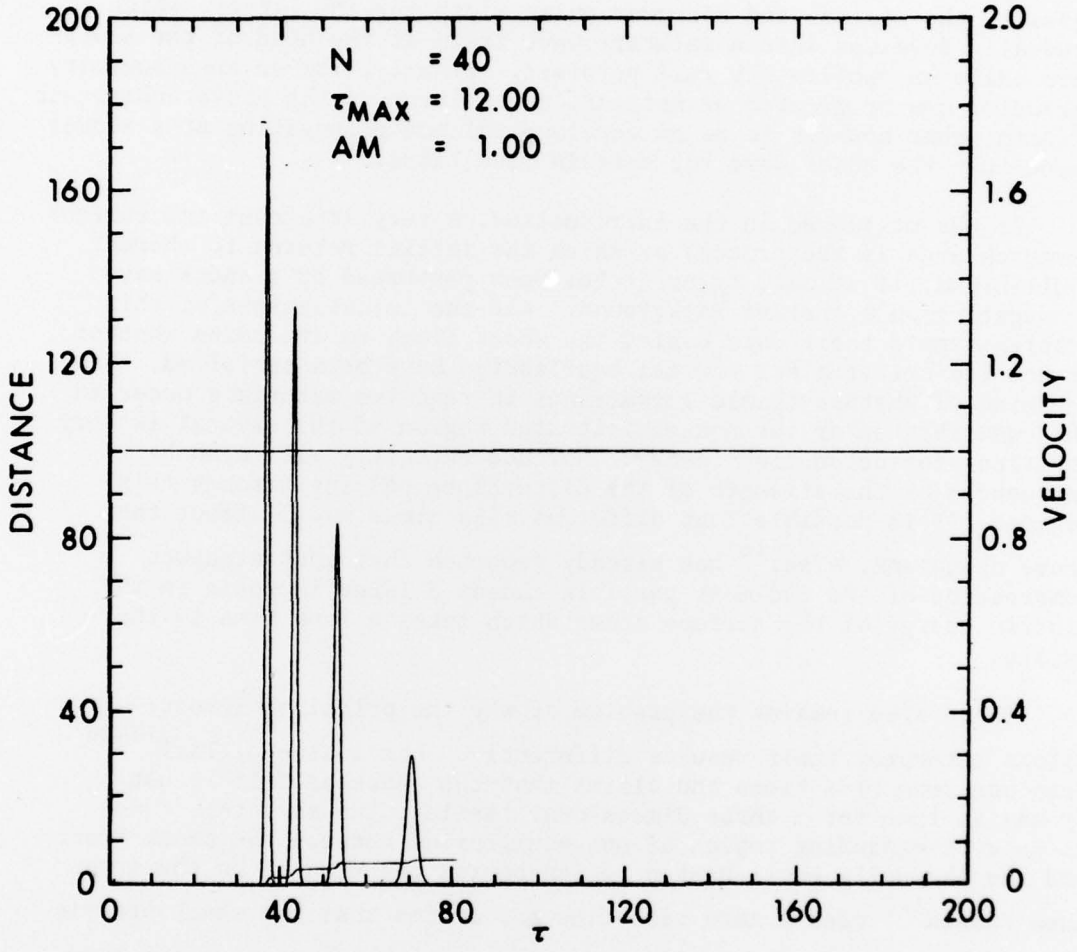

Figure 36. In dimensionless units the velocity which propagates as four solitary waves and the displacement from equilibrium of the 40^{th} particle are plotted as a function of time for a lattice with an anharmonicity parameter A_m=1.0 and deceleration time τ_{max}=12.0. The zeroth particle starts out with initial velocity of unity and is decelerated to zero.

than the corresponding amplitude for the instantaneous compression case by an amount which is inversely proportional to the rise time τ_{max}. As the lattice becomes slightly anharmonic, each amplitude of the successive peaks in the wave train passing through the surface particles behaves in a manner which is analogous to the harmonic case. The most distinguishing factor between the harmonic and slightly anharmonic cases is the steeper and narrower pulse width for the latter, which gradually develops into a solitary wave train at the head of the shock wave while an oscillatory tail persists. Finally, for an anharmonicity parameter one or greater we noticed, in addition to the above anharmonic effects, what appears to be an envelope soliton propagating at a slower speed than the shock wave for certain rise times.

As was mentioned in the introduction, a very important and current research area is the process by which the lattice returns to thermal equilibrium, if at all, after it has been perturbed by a shock wave propagating on a thermal background. All the investigators of this problem sample their data behind the shock front to determine whether or not the criteria for thermal equilibrium have been satisfied. The question of whether chemical reactions in reactive materials occur in the equilibrated or the non-equilibrated region of the crystal is very important for detonation theory. Surface chemistry will also be influenced by the strength of the disturbance passing through this region. It is possible that different rise times could affect the above phenomena. Tsai[16] has already reported that instantaneous compression of the end-most particle causes a large increase in the kinetic energy of the surface atoms which takes a long time to thermalize.

There also remains the problem of why the principal investigators interpret their results differently. For instance, Tsai[14-16] uses non-zero rise times and claims that the shock profile is not steady in time for a three-dimensional lattice. He says that there is an ever-expanding region of non-equilibrium between the shock front and the thermally equilibrated region behind the front. On the other hand Paskin[1-2] uses a zero rise time and claims that the shock profile is steady in time. Powell and Batteh[13] use a zero rise time and have found that the shock profile is not steady in a one-dimensional lattice. Unfortunately, we did not propagate our shock wave on a thermal background in this investigation. However, we feel that the different wave characteristics in the surface atoms, and the possibility of envelope solitons propagating at a slower speed than the shock front, would exist, but would be masked by the thermal background. Therefore, future investigators should be aware of these results as they strive for a uniform interpretation of the shock wave problem.

ACKNOWLEDGEMENTS

We wish to express our appreciation to Dr. J.H. Batteh and Dr. J.D. Powell for many useful technical discussions, as well as the help they gave in modifying their computer program for the anharmonic lattice. We also want to thank Dr. W. Gautschi of Mathematics Research Center, University of Wisconsin, and W.O. Egerland of BRL for discussions which helped us obtain Eq. (3.22). The computational assistance of G. Beck of APG Management Information Systems Support Division is gratefully acknowledged.

REFERENCES

1. A. Paskin and G.J. Dienes, "Molecular Dynamic Simulations of Shock Waves in a Three-Dimensional Solid", J. Appl. Phys. 43, 1605. (1972).

2. A. Paskin and G.J. Dienes, "A Model for Shock Waves in Solids and Evidence for a Thermal Catastrophe", Solid State Comm. 17, 197 (1975).

3. R. Manvi, G.E. Duvall, and S.C. Lowell, "Finite Amplitude Longitudinal Waves in Lattices", Int. J. Mech. Sci. 11, 1 (1969).

4. G.E. Duvall, R. Manvi, and S.C. Lowell, "Steady Shock Profile in a One-Dimensional Lattice", J. Appl. Phys. 40, 3771 (1969).

5. R. Manvi, and G.E. Duvall, "Shock Waves in a One-Dimensional, Non-Dissipating Lattice", Brit. J. Appl. Phys. 2, 1389 (1969).

6. R. Manvi, "Shock Wave Propagation in a Dissipating Lattice Model", Ph.D. Thesis (Washington State University, 1968) (Unpublished).

7. J. Tasi, "Perturbation Solution for Growth of Nonlinear Shock Waves in a Lattice", J. Appl. Phys. 43, 4016 (1972). See also Erratum (J. Appl. Phys. 44, 1414 (1973)).

8. J. Tasi, "Perturbation Solution for Shock Waves in a Dissipative Lattice", J. Appl. Phys. 44, 2245 (1973).

9. J. Tasi, "Far-Field Analysis of Nonlinear Shock Waves in a Lattice", J. Appl. Phys. 44, 4569 (1973).

10. J. Tasi, "Reflection of Nonlinear Shock Waves in a Lattice", J. Appl. Phys. 47, 5336 (1976).

11. M.J.P. Musgrave and J. Tasi, "Shock Waves in Diatomic Chains - I. Linear Analysis", J. Mech. Phys. Solids 24,19 (1976).

12. J. Tasi and M.J.P. Musgrave, "Shock Waves in Diatomic Chains - II. Nonlinear Analysis", J. Mech. Phys. Solids 24, 43 (1976).

13. J. Powell and J. Batteh, "Shock Propagation in the One-Dimensional Lattice", BRL Report No. 2009, USABRL, APG, MD, Aug 1977. (AD #A044791)

14. D.H. Tsai and C.W. Beckett, "Shock Wave Propagation in Cubic Lattices", J. Geophys. Res. 71, 2601 (1966).

15. D.H. Tsai, "An Atomistic Theory of Shock Compression of a Perfect Crystalline Solid", in Accurate Characterization of the High-Pressure Environment, edited by E.C. Lloyd, Natl. Bur. Stds. Spec. Publ. No. 326 (U.S. GPO, Washington, DC, 1971), p. 105.

16. D.H. Tsai and R.A. MacDonald, "Second Sound in a Solid Under Shock Compression", J. Phys. C, 6, L171 (1973).

17. H. Prask, P. Kemmey, S. Trevino, D.H. Tsai, and S. Yip, "Computer Simulation Studies of the Microscopic Behavior of Shocked Solids", Proceedings of the Conference on Mechanisms of Explosion and Blast Waves, editor J. Alster (JTCG/ALNNO, Naval Weapons Station, Yorktown, VA, 1973, XVI).

18. W. Band, "Studies in the Theory of Shock Propagation in Solids", J. Geophys. Res. 65, 695 (1960).

19. D.R. Bland, "On Shock Structure in a Solid", J. Inst. Math. Applications 1, 56 (1965).

20. E. Fermi, J.R. Pasta, and S.M. Ulam, "Studies in Nonlinear Problems", Los Alamos Sci. Lab. Rep. LA-1940, 1955; also in Collected Works of Enrico Fermi (Univ. Chicago Press, Chicago, 1965), V. II, p. 978.

21. B. Lewis and G. von Elbe, Combustion, Flames and Explosion of Gases (Academic Press, New York, 1951), Chap. XI.

22. E. Schroedinger, "Zur Dynamik Elastisch Gekoppelter Punktsysteme", Ann. Phys. 44, 916 (1914).

23. P.M. Morse and K.U. Ingard, Theoretical Acoustics (McGraw-Hill, New York, 1968), Chap. 3.

24. Handbook of Mathematical Functions, edited by M. Abramowitz and I. Stegun (Natl. Bur. Std., WASH, DC, 1964), Chap. 9.

25. W. Kapteyn, "Sur Quelques Integrales Definies Contenant Des Fonctions De Bessel", Archives Neerlandaises Des Sciences Exactes et Naturelles, VI, 103 (1901).

26. W. Gautschi, private communication.

27. B. Carnahan, H.A. Luther, and J.O. Wilkes, Applied Numerical Methods (Wiley, New York, 1969), Chap. 6.

28. N.J. Zabusky, "Solitons and Bound States of the Time-Independent Schrodinger Equation", Phys. Rev. 168, 124 (1968).